ISAS - INTERNATIONAL SCHOOL FOR ADVANCED STUDIES

Mechanisms of control and modulation of the GABAergic system in the rat hippocampus.

Thesis Submitted for the degree of
Doctor Philosophiæ

Candidate
Marco Atzori

Supervisor
Prof. Andrea Nistri, M.D.

December 1995

SISSA - SCUOLA INTERNAZIONALE SUPERIORE DI STUDI AVANZATI
TRIESTE
Strada Costiera 11

TRIESTE

All the experiments and the data analysis performed during this work were carried out by the candidate in the Laboratories of Biophysics at SISSA.

Part of the work presented here was published or submitted for publication:

Pyramidal cells and Stratum-Lacunosum-Moleculare interneurons in the CA1 region of the hippocampal region share a GABAergic spontaneous input.
Marco Atzori, submitted.

Effect of Thyrotropin Releasing Hormone on GABAergic transmission of the rat hippocampus.
Marco Atzori and Andrea Nistri, submitted.

Cl^- transporter block enhances GABAergic spontaneous activity in rat hippocampal CA3 cells.
Marco Atzori, NeuroReport 5, 2509-2512 (1994).

Content

List of abbreviations

$[\ ]_i$	intracellular concentration
$[\ ]_o$	extracellular concentration
5-HT	5-hydoxytriptamine
CA1,2,3	Cornu Ammoni area 1,2,3
CCT	Chloride Cation Transporter
CNS	Central Nervous System
CTB	Cl^--Cation-Transporter-Blocker
DG	Dentate Gyrus
ePSC	evoked Post Synaptic Current
GABA	γ-amino-butyric acid
$GABA_AR$	$GABA_A$ Receptor
GAD	Glutamate Decarboxylase
GIN	GABAergic Interneuron
Glu	Glutamate
mPSC	miniature Post Synaptic Current
NMDA	N-methyl-D-Aspartate
O-A	Oriens-Alveus
PC	Pyramidal Cell
PN	Post-Natal
PSC	Post Synaptic Current
SL-M	Stratum Lacunosum-Moleculare
SP	Stratum Pyramidale
sPSC	spontaneous Post Synaptic Current
SR	Stratum Radiatum
t-ACPD	trans-1-aminocyclopentane-1,3-dicarboxilic acid
TRH	Thyrotropin Releasing Hormone
TTX	Tetrodotoxin
V_r	Resting potential
E_{Cl^-}	Cl^- reversal potential
EGTA	Ethyleneglycol-tetraacetic acid

SUMMARY

The whole-cell patch-clamp technique was used to investigate the properties of GABAergic synaptic transmission in thin slices of rat hippocampus and its sensitivity to pharmacological modulation. Spontaneous GABAergic synaptic events recorded from pyramidal cells (PCs) of Stratum Pyramidale (SP) were compared with those recorded from the interneurons of Stratum-Lacunosum Moleculare (SL-M IN) in the CA1 region. GABAergic spontaneous activity displayed similar frequency (0.75±0.26 Hz vs. 0.53±0.11 Hz), amplitude (34.6±5.0 pA vs. 39.6±4.1 pA), rise-time (2.9±0.4 ms vs. 3.2±0.3 ms) and decay-time (31.7±1.5 vs. 32.3±2.4) in PCs or SL-M INs, respectively. Various pharmacological agents were bath-applied to induce changes in the frequency of spontaneous postsynaptic currents (sPSCs). sPSC frequency increased after furosemide, carbachol, trans-1-aminocyclopentane-1,3-dicarboxilic acid (t-ACPD) or l-arg, whereas it decreased after 5-hydroxy-tryptamine (5-HT) or baclofen in either class of cells. Double patch recording from one pyramidal cell and one SL-M IN revealed a number of simultaneous events 4.4 times larger than the number of randomly occurring coincidences, as detected by cross-correlation analysis. The ratio between measured and random coincidences did not vary when the sPSCs frequency was increased. These results suggest that a single class of yet unidentified spontaneously active GABAergic cells impinged on PC and on SL-M interneurons exerting an overall control on PC and on SL-M IN through release of GABA.

The effect of Thyrotropin Releasing Hormone (TRH), a neuropeptide physiologically present in the mammalian hippocampus, on spontaneous, miniature and evoked GABAergic postsynaptic currents (PSCs) was investigated by recording from pyramidal cells and interneurons. Bath-application of 10 μM TRH induced an increase in the frequency of sPSCs currents from 1.07±0.68 Hz to 3.16±0.73 Hz in pyramidal neurons and interneurons of the Stratum Lacunosum Moleculare (SL-M). In tetrodotoxin (TTX) solution TRH did not change miniature PSCs. Application of TRH to mini-slices containing the CA1 region only, still produced an increase in the sPSC frequency, indicative of an action by TRH upon a

local GABAergic circuitry. In a small subset of cells TRH induced the appearance of highly rhythmic large PSCs at a frequency of about 2 Hz as confirmed by autocorrelation analysis. Averaged PSCs evoked by focal stimulation of the SL-M region were depressed (from 90±27 pA to 44±15 pA) after application of TRH. This phenomenon was solely due to an increase in the number of synaptic failures. It is proposed that the effect of TRH on the GABAergic system was primarily exerted on a subset of interneurons controlling the activity of pyramidal cells as well as SL-M interneurons.

Chloride-cation-Transporter-Blockers (CTBs) furosemide and ammonium were used to test the effect of changes in the internal [Cl^-] on the spontaneous and miniature GABAergic PSCs of CA3 pyramidal cells. CTBs application in the presence of kynurenic acid raised (65±21%) the frequency of GABAergic spontaneous PSCs leaving unchanged the miniature frequency, indicating that the increase in synaptic activity was presynaptically caused by interneuronal firing. Partial removal of external chloride yielded the same effect, suggesting that E_{Cl}^- contributes to the resting potential of interneurons. Furosemide prolonged PSC risetimes while PSC mean amplitude and the response to exogenous muscimol were decreased, thus confirming that this agent produces some $GABA_A$ receptor antagonism.

Chapter 1

Introduction

1.1 Synaptic inhibition in the brain

The nervous system connects different parts of the animal body and coordinates its activity. A major function of the nervous system is to process incoming sensations and to elaborate a behavioural output. This can be accomplished using three different types of unit: sensory neurons, that translate the energy of relevant stimuli into coded impulses, output units such as motor neurons producing muscle contraction after nerve impulses, and interneurons, constituting the intermediate processing device. While sensory and output neurons work essentially as excitatory devices since the earliest steps in evolution, nature endowed the interneuronal machinery of inhibitory as well as excitatory units, allowing tuning of behaviour through fine shaping of excitatory signals. Particularly in vertebrates, the high degree of divergence of excitatory pathways introduces the need for limiting the spread of excitation to mantain motor activity under control. Inhibition can be defined as any

physiological process counteracting cellular excitation. Different mechanisms are used to implement inhibition in the Central Nervous System (CNS).

1.2 Mechanisms of synaptic inhibition

Several mechanisms may dampen cellular excitability. A negative current may shift resting potential towards more negative values moving it away from the firing threshold. Inflow of negative charges or outflow of positive charges are two possible ways of obtaining a negative current. Inhibitory channels directly opened by ligands use mainly the first process while voltage-activated intrinsic channels are often responsible for the second one. A further mechanism for inhibition is to decrease synaptic transmission by lowering cell membrane resistance, so-called shunting inhibition, either presynaptically or postsynaptically (Frank and Fuortes, 1957). If a negative current is associated with an increase in cell conductance the inhibitory effect is maximal. The increase in cell conductance accompanied by inflow of negative charges is indeed a widely distributed inhibitory mechanism. While in the spinal cord the amino acid glycine is the main inhibitory transmitter (Betz, 1992), in the brain a central role is played by another aminoacid, namely γ-amino-butyric acid (GABA; reviewed in Sivilotti and Nistri, 1991; Kaila, 1994). As for several other neurotransmitters, ionotropic as well as metabotropic membrane receptors do exist for GABA (Bowery et al., 1980). Ionotropic GABA channels are permeable essentially to chloride ($GABA_A$ receptor) whereas metabotropic receptors seem to lead to K^+ channel opening (Newberry and Nicoll, 1984). We will focus our attention to $GABA_A$ receptor activation. GABAergic interneurons (GINs) are recognizable with immuno-histochemical, morphological and electrophysiological techniques. GINs are mostly confined to local networks although important projection tracts are GABAergic as well. Here the main features of inhibition through the so-called $GABA_A$ receptor are rapidly reviewed.

1.3 The $GABA_A$ receptor

In the adult mammalian brain the $GABA_A$ receptor ($GABA_AR$) is a multimeric protein complex which belongs to the superfamily of ligand-gated ion channels (Olsen and Tobin, 1990; Smith and Olsen, 1995). It is made up of 5 subunits: two α, and one β, γ and δ (Wisden and Seeburg, 1992). It is characterized by its permeability to Cl^- (Krnjevic and Schwartz, 1967; Barker and Ransom, 1978), by the sensitivity to the competitive antagonist bicuculline, and to the agonists muscimol and isoguvacine (Macdonald et al., 1992). Moreover, it is allosterically modulated by benzodiazepines, barbiturates and steroids (Macdonald et al. 1992; Maiewska, 1992). At the single channel level it displays a conductance in the range 23-30 pS (Macdonald et al., 1992; Kaila, 1994). $GABA_AR$ presents binding sites for Zn^{2+}, Ca^{2+} and for phosphorilation (Macdonald et al., 1992; Stelzer, 1992). Like the majority of the ligand-gated channels $GABA_AR$ (after agonist binding) develops desensitization, namely gets temporarily into a closed state, refractory to further opening. Its desensitization is faster at more negative transmembrane voltage and with high $[Ca^{+2}]_i$ (Frosch et al., 1992; Hablitz, 1992; Gage and Chung, 1994). A growing number of variants of $GABA_AR$ subunits has been cloned although the basic features of the $GABA_AR$ do not seem to vary greatly from invertebrates to mammals. $GABA_ARs$ can be found virtually in every region: basal ganglia (Bernardi et al., 1976), cerebellum (Eccles et al., 1967; Krnjevic, 1982; Vincent and Marty, 1993), retina (Müller et al.,1992), primary sensory areas (Kisvárday et al., 1993) and motor cortex (Branch and Martin, 1958; Krnjevic, 1964), thalamus (Purpura and Cohen, 1963) and hippocampus (Alger and Nicoll, 1980). Three ions are particularly abundant in the nervous tissue of mammals: Na^+, K^+ and Cl^-. Since Na^+ and K^+ are used for action potential signalling by voltage gated conductances and for synaptic excitation by non-selective cationic channels it is not surprising to notice that nature developed an independent mechanism for inhibition based on Cl^- . Cl^- membrane transporters (Babila, 1989; Zhang et al., 1991) and probably an inwardly rectifying chloride conductance (Staley, 1994)

keep constantly low intracellular Cl^- concentration $[Cl^-]_i$ with respect to the external one $[Cl^-]_o$, with the result that the Nernst potential for Cl^- is near the resting cell potential or even more negative. This in turn yields the effect that Cl^- currents are normally inhibitory because they are due to inflow of negative charges and accompanied by a large increase in membrane conductance. Although these properties apply to a wide a range of cells, the situation is slightly more complicated in the developing rat brain.

1.4 The Hippocampus

The mammalian hippocampus is a suitable structure for unravelling the characteristics of the GABAergic system and the modulation of its excitability. The discovery that the hippocampal functional unit is the "*lamella* " (slice), unlike the neocortex which is organized in columns, greatly helped physiologists and anatomists in starting a series of investigations which often represented pioneer experiments giving general insight into the CNS. The hippocampus can in fact be cut in slices perpendicularly to the axis of its elongation (*transverse* slice) with minimal loss of functional synapses. The wealth of well established anatomical, morphological, biochemical and physiological data available for this area has provided a relatively detailed knowledge of the basic principles of cellular function within an essentially preserved neuronal circuitry. Minimal variations in the anatomy of hippocampus of different mammalian species are reported from rat to man as expected for a phylogenetically old part of the CNS. The hippocampus makes up a relatively self-contained information processing region receiving and projecting axons from the subiculum. Three main different regions are cytoarchitectonically distinguishable in the hippocampus: a region (Dentate Gyrus, DG) whose principal neurons are granule cells, and two adjacent regions around Ammon's horn (Cornu Ammoni), CA1 and CA3, whose principal cells are pyramidal shaped. In

primates an intermediate region (CA2) separates the last two. The tissue surrounding the pyramidal cell layer contains a relatively low density of cell bodies and one or more parallel bundles of axons. At the outer hippocampal surface, Oriens-Alveus (O-A), it is much thinner than in the inner side, Stratum-Lacunosum Moleculare (SL-M). Backbone of the hippocampal circuitry is an excitatory trisynaptic pathway that connects the input from high level sensory areas to the granule cells of the Dentate Gyrus. Dentate Gyrus granule cells send their axons (mossy fibers) to CA3 pyramidal cells which in turn project to CA1 pyramidal cells with the Schaffer collaterals. In addition a direct projection to both CA3 and CA1 is sent from the perforant path while a recurrent collateral of the bifurcated axons from CA3 pyramidal cells feeds forward the CA3 region itself. It is widely accepted that the all the synapses described above are excitatory and use the amino-acid glutamate (Glu) as neurotransmitter (Bernard and Wheal, 1994).A scheme for the basic hippocampal slice circuitry is shown in fig. 1.

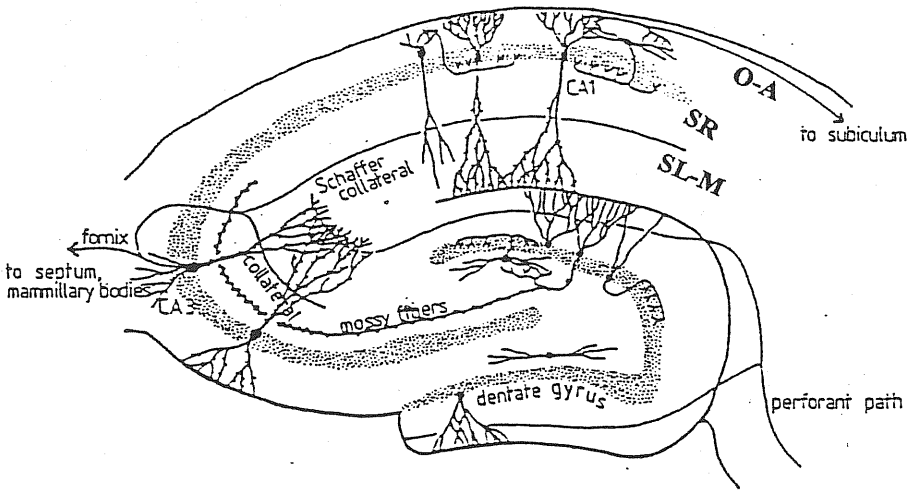
CA1
O-A
SR
SL-M
to subiculum
Schaffer collateral
fornix
to septum, mammillary bodies
CA3
collateral
mossy fibers
dentate gyrus
perforant path

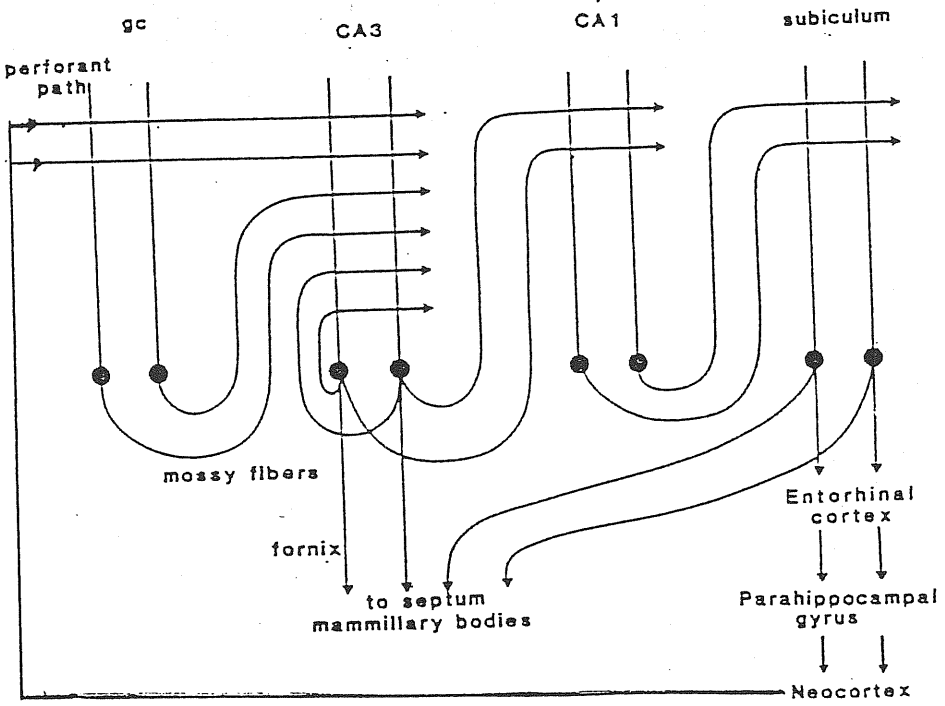
gc
CA3
CA1
subiculum
perforant path
mossy fibers
fornix
to septum
mammillary bodies
Entorhinal cortex
Parahippocampal gyrus
Neocortex

Fig.1. The trisynaptic excitatory circuit of hippocampus.

Above: granule cell of the Dentate Gyrus receive an excitatory input from the perforant path projecting their excitatory axons to CA3 pyramidal cells *via* the mossy fibers. CA3 pyramidal cells receive also a direct input from the perforant path and send an excitatory input to CA1 pyramidal cells through the Schaffer collaterals. CA1 pyramidal cells send their axons to the subiculum. The pyramidal cell layer is surrounded by the Oriens-Alveus (O-A) on one side and by the Stratum Radiatum (SR) and Stratum Lacunosum Moleculare (SL-M) on the other side.

Below: neocortex is both a main afferent and efferent area for hippocampal cells. In fact, the neocortex infact sends its output to the hippocampus through the perforant path and receives information from it through the entorhinal cortex (from Rolls et al., 1993).

Besides the main excitatory backbone, the hippocampus receives an important input via fornix/fimbria , a major myelinated afferent boundle entering the medial aspect of the CA3 region. Among the fimbrial axons, most relevant are those coming from septal diagonal band of Broca, using acetylcholine and GABA as transmitters, from Raphe's nucleus using serotonin, and other ones using monoamines, opioids, steroids and oligopeptidic hormones. Such inputs are believed to exert a modulatory influence on the tri-synaptic circuit rather than directly driving its activity. The fimbria also contains hippocampal efferent fibers to the same regions indicated above. A box diagram of the main hippocampal afferents/efferents is shown in fig. 2.

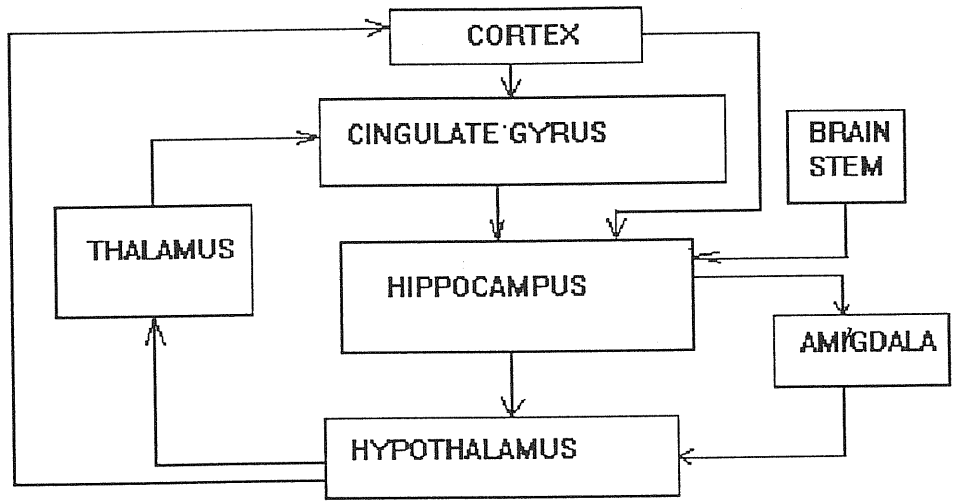

Fig.2: box diagram of hippocampal connections. The hippocampus is a part of the so-called limbic system which includes hypothalamus, amygdala, cingulate gyrus and thalamus.

1.5 GABAergic interneurons in the hippocampus

GABAergic interneurons were identified in the hippocampus on the basis of their positive immunohistochemical response to antibodies against the GABA-synthesizing enzyme, Glutamate Decarboxylase (GAD), or to the Ca^{2+} binding enzymes calbinding and parvalbumin, considered as markers of GINs (Gulyás et al, 1990; Kawaguchi and Hama, 1987; Kunkel et al., 1988). The presence of symmetrical synapses is also considered to be associate with GINs (Ribak et al., 1978).

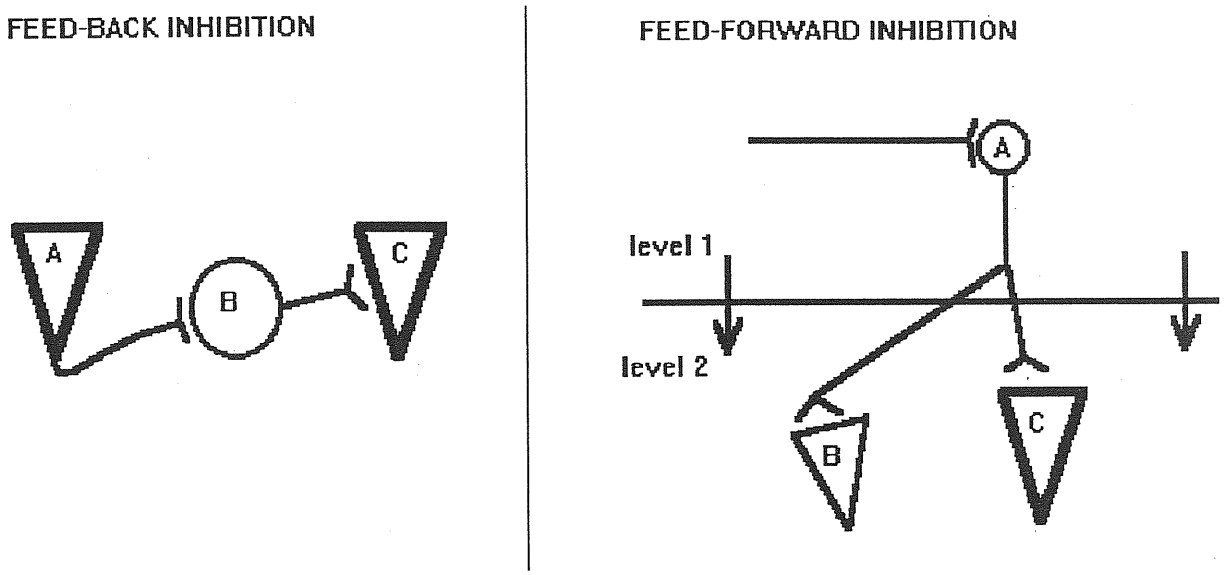

Fig.3 Inhibitory circuits: feed-forward inhibition is sent from a processing level (A) to a different one (B) while feedback inhibition functionally links an excitatory cell (A) to other cells (B and C) of the same level.

On the postsynaptic membrane, binding studies using GABA, the $GABA_A$ agonist muscimol and the $GABA_A$ blocker bicuculline, confirmed the presence of GABA-sensitive sites, as also shown by

electrophysiologic means. In principle, each one of the cell types described above can receive an inhibitory input driven either by feed-forward or from feed-back GINs as schematically depicted in fig.3.From a morphological point of view a dozen of different GINs have been identified although a simplified classification restricts them to three classes readily recognizable with optical methods in the in vitro preparation: interneurons of the O-A (O-A INs), interneurons of the Stratum Pyramidale (SP INs) and SL-M interneurons (SL-M INs). In particular pyramidal cells of the hippocampal CA1 region of the young rat receive a spontaneously active GABAergic drive (Ropert et al. 1990) whose functional meaning is still unknown. It is not clear whether GABAergic spontaneous events are an exclusive feature of pyramidal cells or, on the contrary, non-pyramidal cells in CA1 receive a spontaneous input as well. Spontaneous postsynaptic currents (sPSCs) are considered as markers of synaptic connection for helping to unravel hippocampal interneuronal circuitry. Interneurons in the Stratum Lacunosum Moleculare (SL-M) or inner border of Stratum Radiatum are well studied both from the morphological and electrophysiological point of view (Lacaille and Schwartzkroin, 1988 a and b, Williams and Lacaille 1992, Williams et al. 1994, Kunkel et al. 1988). To the best of our knowledge., no information is available concerning a common input from any class of interneurons to different types of hippocampal cells. This would allow us to improve the understanding of the hippocampal circuitry and possibly to envisage new functional implications. Since in pilot experiments SL-M interneurons displayed spontaneous synaptic GABAergic activity, in the present project they were compared with pyramidal cells. Different types of hippocampal interneuron could be subjected to differential modulation by neurotransmitters. Metabotropic agonists for glutamate, GABA and acetylcholine and serotonin receptors were used in order to modulate sPSCs. Direct evidence for a common input would be provided by comparing sPSCs appearing simultaneously on a cell of each class.

1.6 Modulation of synaptic transmission by neuropeptides

Several neuropeptides are known to affect neuronal excitability through different cellular mechanisms. The tri-peptide Thyrotropin Releasing Hormone (TRH) present in the hypothalamus elicits the hypophyseal secretion of thyrotropin, which in turn induces thyroxine release from the thyroid. Beside its effect on the endocrine system TRH also affects neurotransmission. The neuropeptide is indeed found in relatively high concentration in the hippocampus (Sharif, 1989). Its distribution and receptor binding sites have been widely investigated (Manaker et al., 1985; Low et al., 1989; Eymin et al., 1993). Nevertheless, the function of TRH remains still unknown. Since TRH has been shown to exert slow modulatory effects on brainstem (Reckling, 1990) and spinal neurons (Bayliss et al., 1992; Fisher and Nistri 1993), attention has recently been payed to the possibility that TRH might exert a modulatory role in the hippocampus as well. Within this framework it has been shown that TRH mimicks the action of serotonin in depressing a high threshold Ca^{2+} dependent K^{+} conductance (Ballerini et al., 1994) and that it selectively enhances glutamatergic transmission mediated by N-methyl-D-aspartate (NMDA) receptors (Stocca and Nistri, 1994, 1995) in analogy to the phenomenon reported in the cerebral cortex (Kasparov et al., 1994). The mechanism through which TRH produces these effects is unclear, but in analogy to the well documented effect of this peptide on phosphoinositol metabolism of cultured pituitary cells (Gershengorn, 1986) it has been suggested that a similar phenomenon may take place in hippocampal neurons (Ebihara and Akaike, 1993). Should this be the case one might expect that other neurotransmitter pathways might be susceptible to a modulatory action by TRH. In particular, inhibitory neurotransmission mediated by GABA has not been thoroughly investigated for its sensitivity to TRH.

1.7 $GABA_A$ and $[Cl^-]_i$ in immature rat brain.

Pyramidal cells in the hippocampal CA3 region of neonatal rats receive a major input directly from local GABAergic interneurons (Hosokawa et al., 1994). The interneurons themselves also receive a large GABAergic afference (Lacaille et al., 1989). The transmembrane chloride gradient is regulated by several mechanisms like movement of Cl^- through leak channels and active and passive Cl^- transport (Cherubini et al., 1991; Misgeld et al., 1986). In the rat hippocampus $[Cl^-]_i$ is controlled by chloride transporters among which the most relevant seems to be the so-called Chloride-Cation Transporter (CCT), which also involves Na^+ and K^- (Thompson et al. 1988a,b). A higher $[Cl^-]_i$ would explain why in neonatal pyramidal cells or in adult dentate gyrus GABA elicits membrane depolarization (Ben Ari et al., 1989; Ito and Cherubini, 1991) whereas in adult pyramidal cells GABA elicits the usual inhibitory effect. Developmental changes in the $[Cl^-]$ gradient have been particularly studied in pyramidal cells of the CA1 region of the neonatal hippocampus (Zhang et al., 1991). Little is known about the role of $[Cl^-]_i$ in interneuronal activity. The influence of $[Cl^-]_i$ on the spontaneous GABAergic activity generated by interneurons in the CA3 region of the neonatal hippocampus was thus investigated in the course of the present project. Furosemide and ammonium ions were used in order to change $[Cl^-]_i$ since they are known to block the activity of Chloride-Cation-Transporter (CCT) in thick hippocampal slices (Misgeld et al., 1986), in hippocampal organotypic cultures (Thompson and Gahwiler, 1989) and in other CNS preparations (Misgeld et al., 1986; Hall et al., 1989; Nicoll, 1978).

1.8 Aims of the present investigation

This work addressed various issues:

a) What are the characteristics of spontaneous GABAergic activity recorded in different areas of the hippocampus and from different cell types ?

b) Do different types of neuron share an inhibitory input with common features ?

c) Do two cells of different type receive inputs from the same neuron?

d) Is there a common pharmacological modulation of the spontaneous GABAergic input to pyramidal cells and interneurons ?

e) Do TRH affect $GABA_A$-receptor-mediated synaptic transmission ?

If this is the case,

f) does TRH affect $GABA_A$-receptor-mediated spontaneous synaptic transmission ?

g) does TRH affect $GABA_A$-receptor-mediated evoked synaptic transmission ?

h) is the effect of TRH related to a presynaptic or postsynaptic action of the peptide ?

i) are TRH-sensitive neurons present in the same region of their target cells ?

j) what is the influence of $[Cl^-]_i$ on spontaneous GABAergic release generated by interneurons in neonatal hippocampus ? In more detail

does $[Cl^-]_i$ contribute to the resting potential of GABAergic interneurons ?

Since blockers of the Cl^- pumps were used to examin this questions, it was also important to test if Cl^- pump blockers had other presynaptic or postsynaptic effects on GABAergic activity ?

Electrophysiological experiments were performed in order to answer at least partially to these questions.

Chapter 2

Methods

2.1 The hippocampal thin-slice preparation

Relatively recent technical progress endowed electrophysiologists with a new instrument which for the first time allows to use high-resolution patch-clamp directly on whole pieces of nervous tissue, so-called brain thin-slices (Edwards et al., 1989). The technique introduces several advantages with respect to the traditional use of patch clamp of neuronal cell cultures. Synaptic connections at a local level may be at least partially conserved. Furthermore, gene expression and other physiological properties greatly vary in cell cultures from the source tissue, whereas this is unlikely in acutely removed brain tissue. The usual size of thin-slices allows the quite rapid diffusion of bath-applied substances. The dilution of second-messengers in the patched postsynaptic cell is the price to be paid for the high electrical resolution. Slices were obtained from locally bred Wistar rats. Animals (6 to 14 days-old) were anaesthetized with a solution of 5% urethane and decapitated. The brain was immersed in low temperature (2-4 °C), oxygenated (95% O_2, 5% CO_2) Krebs medium inside a Petri dish where the two hemispheres were separated by a scalpel blade. After removal of the cerebellum a

brain emisphere was then layed on his medial surface and cut further to partially remove its parietal aspect as indicated in fig. 4.

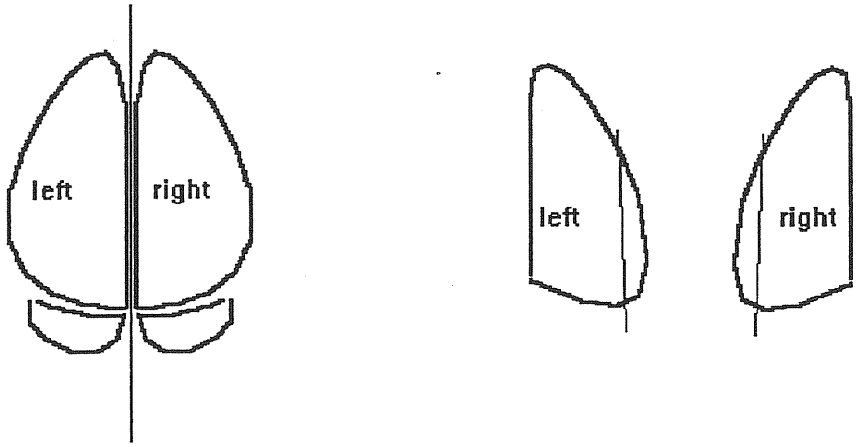

Fig.4. Brain dissection: the two hemispheres are separated, placed on their medial aspect and cut further along a line indicated in the figure. The surface of the cut is used for glueing the tissue to the vibroslicer.

The rest of the tissue was finally glued to a crystal surface in a cutting chamber whose bottom was previously filled with Krebs solution and frozen. The chamber was then filled with Krebs solution brought as close as possible to its freezing temperature. A magnet on the external bottom surface of the chamber secured it to the cutting motor allowing rotation and thus a precise placement of the brain with respect to the cutting blade. A vibro-slicer (FTB Vibracut 2.0) was used for qualitative control of the forward movement speed and of the width of the horizontal vibration. In addition, a manually-adjusted dial gauge allowed to lift the chamber in 10 μm steps. A nominal thickness of 280-350 μm was used for slicing depending on the animal age and on the brain size. Slices were used only when it was possible to discern by eye the presence of the typical hippocampal structure. In

some cases mini-slices were cut from the whole hippocampal slice after removing the dentate gyrus, or the CA3 area (or both) with a scalpel blade. The slices were removed and temporarily placed in a 10-cm-o.d. bell-shaped glass container, filled with Krebs solution under which a resin filter allowed the oxygenating mixture to bubble the Krebs solution. The whole container was kept at 32°C.

2.2 Solutions, drugs and electrodes

Krebs solution contained (mM) NaCl 126, KCl 3.5, $NaH_2PO_4 \cdot H_2O$ 1.2, $MgCl_2 \cdot 6H_2O$ 1.3, $CaCl_2 \cdot 2H_2O$ 2, $NaHCO_3$ 25, glucose 11. Sodium bicarbonate was 11 mM in the solution at 32°C to keep pH to 7.35. Thin slices were moved to the recording chamber where they were superfused at a constant rate of 2-3 mL/min at room temperature (20-22 °C). Mainly two intracellular solutions were used: a first one with internal Cs^+ to improve the cell resistance and with a high concentration of the Ca^{2+} chelator ethylen-glycole-tetra-acetic acid (EGTA), while a second one used K^+ to allow rapid cell repolarization and thus a normal cell firing under current clamp with a milder Ca^{2+} buffering. These will be referred to as Solution Intra1 and Intra2. They had the following composition (mM):

solution Intra1: CsCl 146, NaATP 1.5, HEPES 10, $MgCl_2$ 2, EGTA 11.

solution Intra2: KCl 126, NaATP 1.5, HEPES 10, $MgCl_2$ 2, EGTA 1.

pH was adjusted at 7.35 with KOH. Osmolarity was brought to 305-315 mOsm with addition of KCl.

Drugs were bath applied via the superfusate and took about 15-20 s to reach the tissue. All substances were stored in stocks 10^2-10^4 times concentrated and finally diluted in Krebs solution. Kynurenic acid (1mM, Sigma) was applied to eliminate the ionotropic glutamatergic drive. Kynurenic acid powder was first neutralized with some drops of KOH, dissolved in distilled water

and titrated with HCl to physiological pH. Bicuculline metachloride ((RBI) was used in concentration 2-20 μM to antagonize $GABA_A$ receptors. Picrotoxin (50-100 μM, RBI) and penicillin-G (2mM, Sigma) were used for the same purpose. Furosemide (0.2-3 mM, RBI) and ammonium (2 mM, Carlo Erba) were used as blockers of Cl^- transport. The tri-peptide pyro-glutamyl-histidyl-proline-amide or Thyrotropin Releasing Hormone (TRH), used in concentrations 3-10 μM, was kindly supplied by Takeda. Carbachol, serotonin, trans-1-aminocyclopentane-1,3-dicarboxilic acid (t-ACPD) and baclofen (Sigma) were used at concentrations of 10 μM.

Patch electrodes of about 3-6 MΩ resistance were pulled with a two-steps LIST vertical puller from borosilicate tubings with 1.5 or 2 mm o.d. . Glass capillaries were previously washed in acetone and their ends rounded on a Bunsen flame to prevent damage to the electrode-holder o-rings. Neither electrode polishing nor coating was carried out.

2.3 The recording apparatus

An Axioscope Zeiss microscope endowed with Nomarski optics and a water-immersion lens (400x total magnification) allowed to inspect the slice, select the region over which to perform the recording and eventually identifying individual cells. The amplifier head-stage was held by a hydraulic water- or oil-filled finely adjustable micro-manipulator (Narashige) which in turn was attached to a courser micro-manipulator (Micro.Control) tightened to an aluminium tower. An antivibration table (Newport) ensured minimal sensitivity to external mechanical movements. A Faraday cage electrically isolated the recording chamber from the surrounding noise sources. Voltage- and current-clamp experiments were performed with EPC-7 amplifiers either in voltage clamp or in current clamp mode. Electrode and seal resistances were assessed by short (50-100 ms) voltage pulses.

Capacitance and series resistance correction were performed using the apposite built-in corrections. Cells with series resistence larger than 30 MΩ were discarded. The amplifier was driven by an input-output control board (Digidata 1200) driven by a personal computer (IBM compatible) with the pClamp 6.0.2 software, either in the continous or in the pulse mode. The basic recording configuration is displayed in fig. 5.

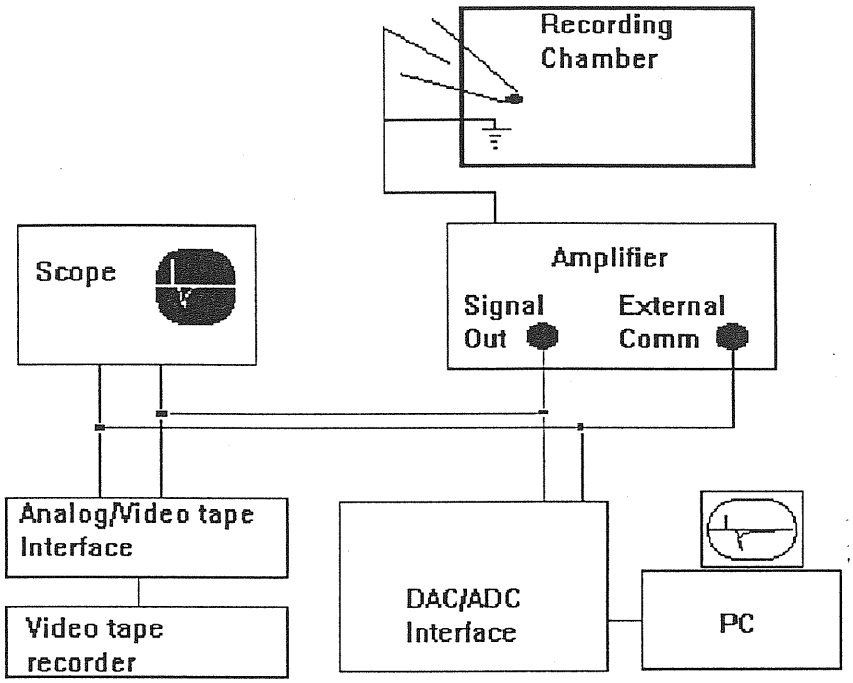

Fig.5. Basic recording apparatus: the basic scheme of recording is shown. The description of the arrangement is reported in the text.

Extracellular focal stimulation was used to evoke postsynaptic potentials. The pClamp driven output trigger was sent to a further trigger generating device (Digitimer 1000) to delay the start of the stimulus with respect to the acquisition itself. The delayed signal was finally sent to an isolated stimulator unit (Digitimer RS2A) used for generate stimuli in the range ± 1-100 V, 10 μs to 1 ms long. Such a procedure allowed a clear identification of the stimulus artifact in the acquired traces.

Stimulation was carried out in the slice by a patch electrode similar to that used for recording but filled with extracellular solution. A ground electrode different from that of the signal amplifier was used for stimulation. The circuit is shown in fig. 6.

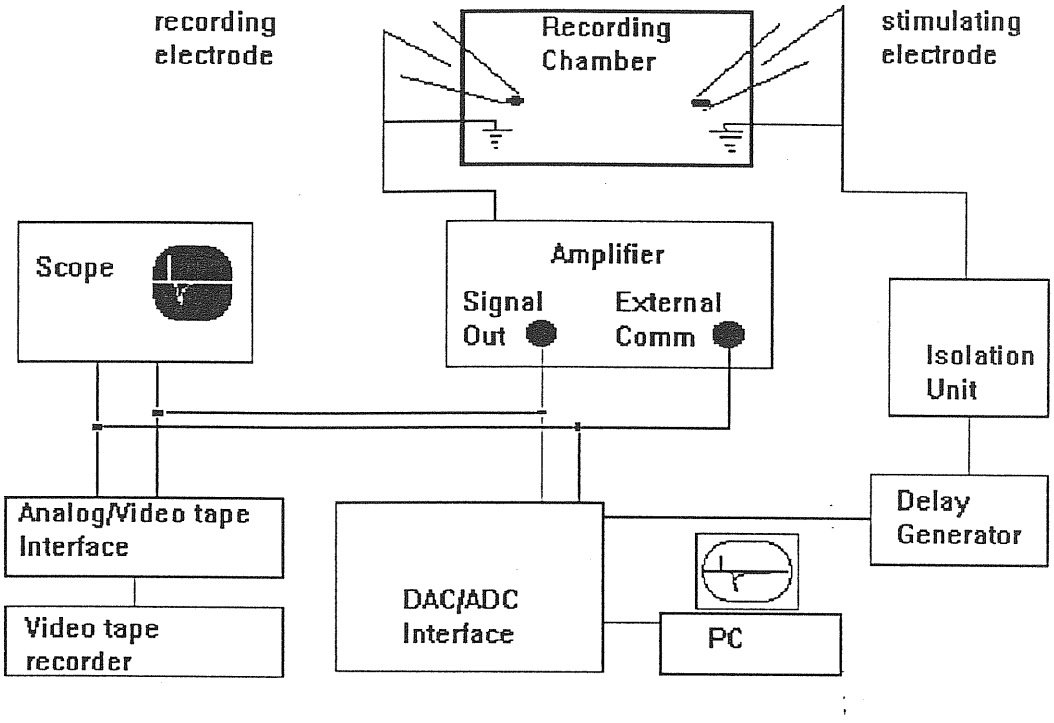

Fig.6. Scheme of the recording apparatus for extracellular stimulation. It is basically the same scheme as in the previous figure with an isolated stimulator unit driven by the trigger of the digitization board through a trigger delay.

In a series of experiments simultaneous patch-clamp recording was performed using two EPC-7 amplifiers. As for single electrode recording with pClamp software it was possible to clamp voltage (or current) on two separate channels as well as to perform digital conversion from two channels at once. A scheme of the connections is given in fig. 7.

During double recording from a pyramidal cell and an interneuron the distance between the two cells was about 100-200 μm.

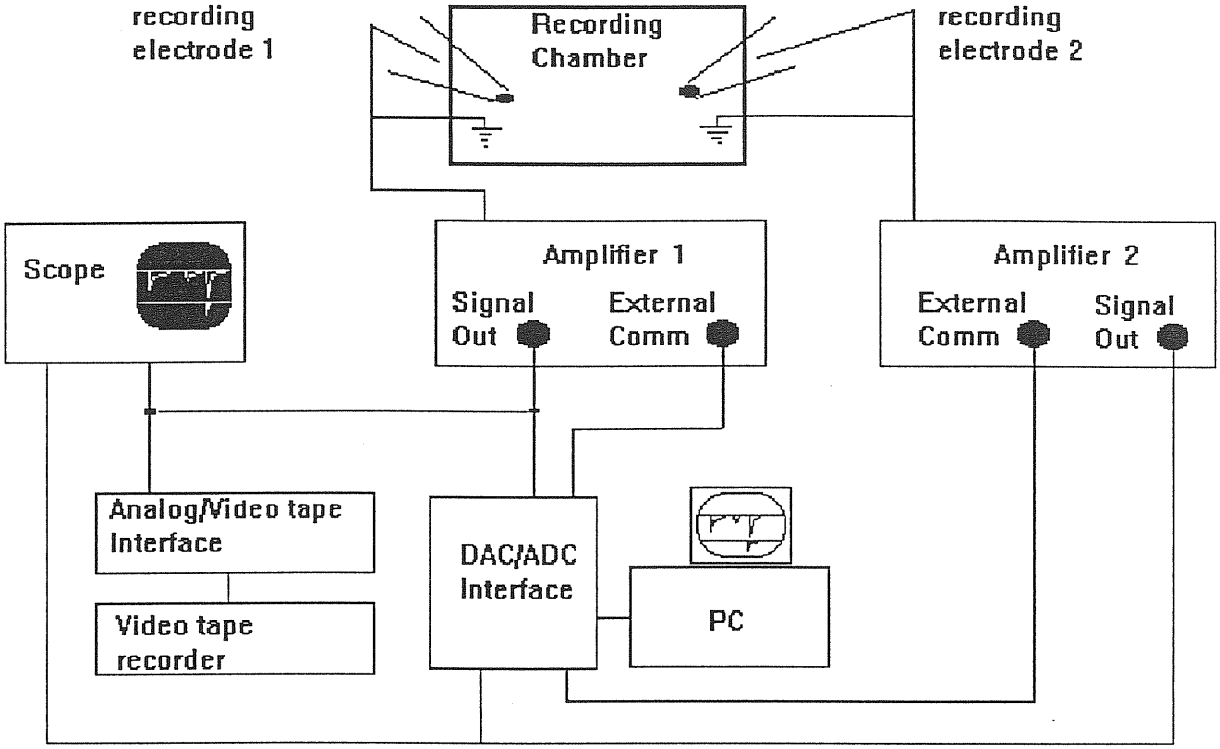

Fig.7. Two-electrode patch-recording. Two-channel patch-clamp recording is performed by taking the output signals from the patch amplifiers (driven by a two-channel DAC board) and recording them on video-tape through a two-channel interface.

Voltage-clamp holding- potential was -70 mV. In current clamp experiments the holding current was selected to mantain the resting potential at about -70 mV. Analog signals were sent to two-channel video tape format interface (Instrutech, VR10B) and then to a videotape (Philips) for recording at 10 kHz sampling rate. The traces were then replayed off-line and digitized at 1-5 kHz after filtering at ½ sampling rate (Electronic device, 8-poles Bessel filter) to eliminate possible signal aliasing. The data were stored on the hard disk of a networked PC before analysis and then backed up onto magnetic tape. Series of 50 responses to extracellular stimulation were often digitized on-line at 4 or 5 kHz sampling rate.

2.4 Data analysis

2.4.1 Spontaneous synaptic activity.

One-channel signals were digitized at 4 kHz and then analyzed with the program N05 generously supplied by Dr. S. Traynelis. Only non overlapping synaptic events were considered for analysis of amplitude, rise-time and decay-time. Frequency was evaluated over 2- to 7-minute-long records. The length of the record was selected in order to get at least about one hundred events per trace. The strategy for analysis of the spontaneous events started with a manual selection of the starting point for the visually detected event, and that was followed by the calculation of the baseline and noise along an interval of 10-50 points before it. The program proceeded to find automatically the starting point as the one when the signal exceeded the noise by more than 50%. The event amplitude was calculated as the difference between baseline and the maximum amplitude evaluated in a preset window (usually 50 points). 20%-80% rise-time analysis supplied the time difference between the related points on the straight line passing through the baseline start of the event and its peak. Single or double exponential fit was performed by using the experimental curve points within a presettable interval selected according to duration of the event as detected by eye. Often GABAergic synaptic events display an exponential decay ending with a plateau followed by a sudden decrease. In such cases exponential function(s) was(were) fitted up to the end of the plateau. A non-linear SIMPLEX algorhythm yielded amplitude and decay-time of the events. For each record an event list was stored in a file containing starting point, amplitude, rise-time and decay-time subsequently used for any further analysis. Event frequency for each record was calculated simply dividing the number of events by the length of the record. In general, results are reported as mean ± s.e.m. unless otherwise stated. Comparisons between different groups were done with paired or unpaired *t*-Student tests, accepting as significant differences with $p < 5\%$.

2.4.2 Evoked postsynaptic currents

Voltage clamp was used to measure postsynaptic currents evoked by electrical stimulation of the afferent fibers. Before each extracellular stimulation a small (5-10 mV) step was applied to constantly monitor cell resistance. The extracellular stimulating electrode, similar to that used for recording, was filled with extracellular solution. Stimulation polarity, length and intensity were varied in order to get stable responses. In particular, stimulation intensity was adjusted to obtain a relatively high percentage of failures (5-50%) to ensure activation of a minimal number of fibers. Tests consisting in series of 50 responses were performed in control conditions, 2-5 min after pharmacological treatment and (whenever possible) after washout. To avoid synaptic fatigue a time lag of 10 seconds separated each acquisition which lasted by itself about 300 ms. Response latencies were evaluated from the start of the stimulus artifact to the start of the corresponding event. A trace was considered as a failure whenever the signal did not exceeded the noise plus 50 %. Mean amplitudes were calculated as the maximum of the averaged responses. Mean amplitudes of the currents were in the range of tens of pA although occasionaly amplitude up to some hundred pA were observed. The variance of the amplitude was calculated the same point. Rise-time and decay-times were calculated as reported above.

2.4.3 Cross correlation analysis

Traces simultaneously recorded from two different cells were digitized at 1 kHz in pulse mode using the maximum allowed window amplitude in order to lose as little interpulse delay as possible with respect to the acquisition time. Traces as long as 800 seconds were acquired in order to get a reasonable large number of correlated events for performing cross-correlation analysis. Two-channel correlation analysis was performed with the help of a home made program written in Basic. To this purpose the i^{th} event was considered as a Dirac delta function at the starting point t_{0i} with integral equal to its amplitude A_i for each function:

$$f_{1,2}(t) = \Sigma_i A_{1,2\,i} \bullet \delta(t - t_{01,2\,i}) .$$

The calculation of the correlation function, defined by the following expression:

$$F(\tau) \equiv \int_{trace} f_1(t') \bullet f_2(t' - \tau)\, dt'$$

becames simply:

$$F(\tau) = \sum_{(ti-tj)=\tau} A_1(t_{0i1}) \bullet A_2(t_{0i2}) .$$

Autocorrelation analysis was performed in some cases using for the autocorrelation function an expression analogous to the above one, obtained by setting:

$$f_1(t) = f_2(t) \quad .$$

Chapter 3

General electrophysiological characteristics of hippocampal cells

Before going into details of the research project the basic cellular electrophysiologic properties of pyramidal cells and interneurons of SL-M were measured and compared with data reported in the literature.

3.1 Membrane properties

3.1.1 Choice of the pipette solution

Since Cs^+-containing intracellular solutions decreases leak conductance the intracellular solution Intra1 was selected whenever experimental objectives allowed it. On the other hand the presence of intracellular Cs^+ also blocks the majority of voltage-gated K^+ channels, preventing development of normal firing patterns. In all cases in which firing pattern analysis was necessary, the solution Intra2 was used.

3.1.2 Pyramidal cells

Cell input resistance was calculated with 60-ms long-pulses of 5-10 mV from a holding potential of generally -70 mV. In CA3 pyramidal cells, using the intracellular solution Intra1 an average input resistance of 202±16 MΩ was measured in control conditions (n=27). The mean resistance of CA1 pyramidal cells in control conditions was 182 ± 32 MΩ with the intracellular solution Intra2 (n=48). The data are comparable for instance with those reported by Williams et al. (237±117 MΩ, 1994) and by Sciancalepore et al. (200-250 MΩ, 1995).

3.1.3 SL-M interneurons

Patch-clamp experiments on interneurons of SL-M were performed in the CA1 region, in which a clear-cut border delimits the cell body region from the inner area. All patch-clamp experiments performed on interneurons were done using the KCl intracellular solution Intra2, in order to observe their firing pattern as stated above. The input resistance of SL-M interneurons in CA1 was 363 ± 92 MΩ, (n=18), significantly higher ($p<0.01$) than that of pyramidal cells. Also in this case the resistance values were comparable with literature data (McBain and Dingledine, 490±30 MΩ, 1993; Williams et al., 352±107 MΩ, 1994).

3.2 Holding potential

Microelectrodes studies report an intracellular resting potential between -60 and -75 mV (Lacaille and Schwartzkroin, 1988b) for pyramidal cells and -58.3±11.3 mV (Lacaille and Schwartzkroin, 1988a) for SL-M interneurons. We wanted to select as a holding potential a value as close as possible to the physiological one, more negative than the activation threshold of low threshold-Ca^{2+}-channels (Carbone and Swandulla, 1989) without substantial activation of the slow inward rectifier current present in pyramidal cells (Halliwell and Adams, 1982). To this end we selected the value of -70 mV.

3.3 Current clamp responses

Different classes of neurons can be classified on the basis of their firing pattern, which is due to the presence of different voltage gated conductances. It is reported (Ashwood et al., 1984; Kawaguchi, 1987) that action potential duration, after-hyperpolarization and firing accommodation differ between pyramidal cells and interneurons in the hippocampus. In particular, interneurons display a pronounced afterhypolarization after each individual spike. In pyramidal cells a long current pulse may elicit no more than 10-15 spikes, unless an interval of some hundred milliseconds is interposed or a strong repolarizing pulse is delivered. On the other hand, in the interneurons the absence of a Ca^{2+}-activated K^+ current with activation rate in the order of hundreds of milliseconds induces the typical non-accommodating firing pattern. Thus, responses to a current pulse of about 1 s were used to provide electrophysiological evidence for the neuronal type. Usually current pulses in the range from 10 to 100 pA elicited sustained spiking, although occasionally current pulses up to 250 pA

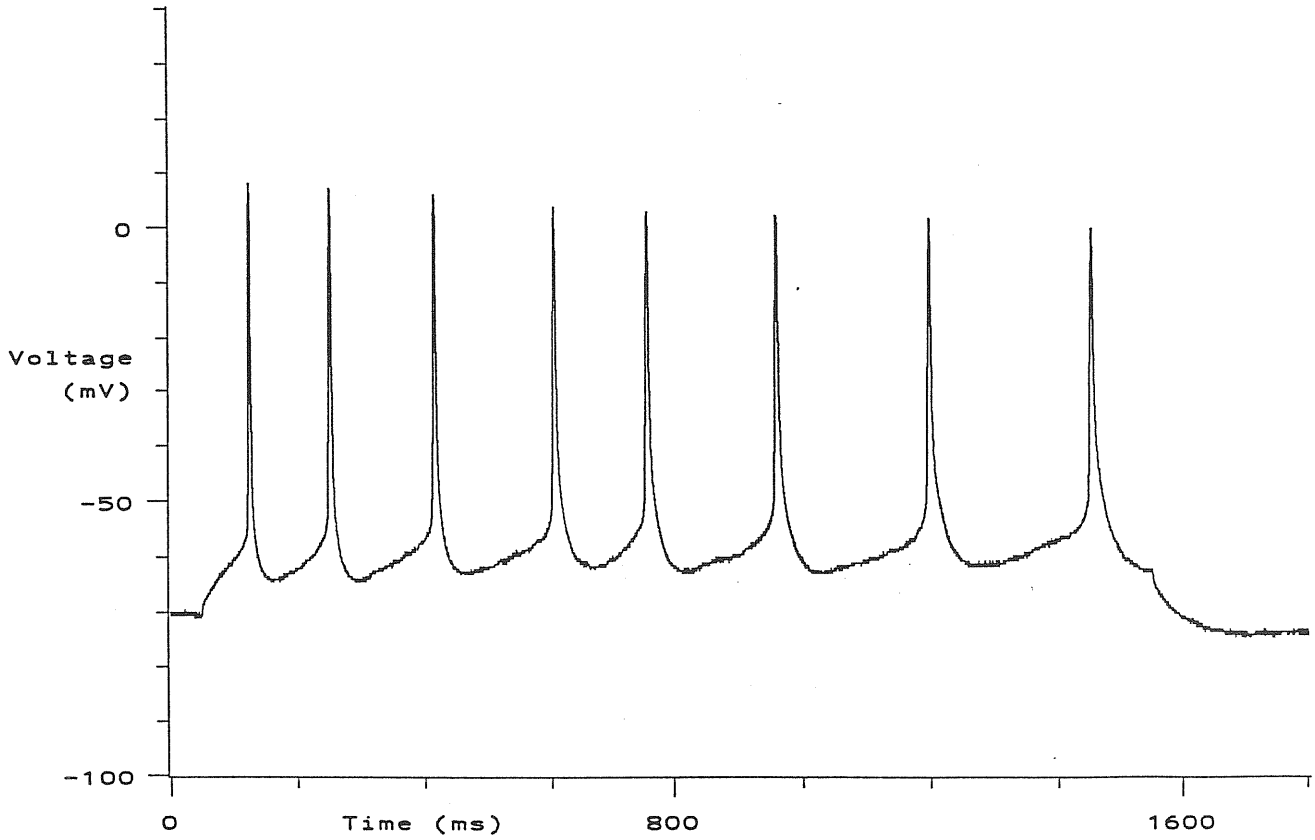
0
Voltage
(mV)
-50
-100
0
Time (ms)
800
1600

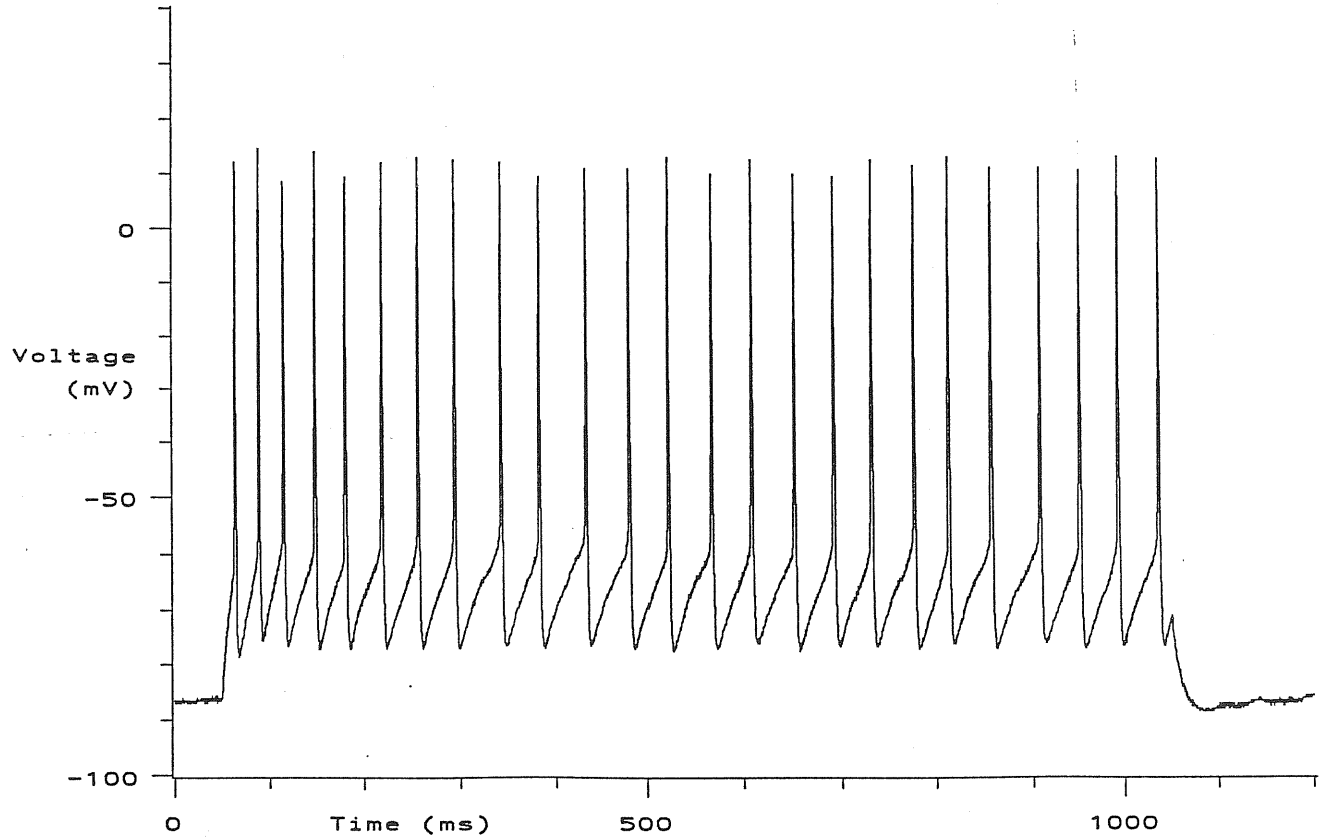
0
Voltage
(mV)
-50
-100
0
Time (ms)
500
1000

Fig.8 Firing pattern of hippocampal cells

Result of the application of a current pulse of 30 pA to a pyramidal cell (above) or to an interneuron in the CA1 region of hippocampus. The length of the pulse is 1500 ms for the pyramidal cell and 1000 ms for the interneuron. In the pyramidal cell the interval between adjacent spikes markedly increases along the pulse, while in the interneuron it stabilizes to an approximately constant value. Notice also the pronounced afterhyperpolarization after each action potential and the shorter action potential width in the interneuron.

Spontaneous PSCs, recorded in the presence of the glutamate-receptor blocker kynurenic acid (1mM), were abolished by 10 μM bicuculline methacloride.

were delivered. In fig.8 it is reported an example of the firing pattern of a CA1 pyramidal cell (above) and of a CA1 SL-M interneuron (below).

3.4 Synaptic activity

The characteristics of postsynaptic GABAergic currents observed in the present project are compared with those reported in the literature. Straightforward comparison is often difficult because of different experimental temperature.

3.4.1 Spontaneous synaptic activity

Ropert et al. (1990) analyzed GABAergic sPSCs in the hippocampal CA1 region at 25°C reporting a value of 3.1 ms for the time-to-peak and a mono-exponential decay time in the range of 21-28 ms. Hosokawa et al. (1994) reported for the decay time a value of 29±4 ms for sPSCs recorded from CA3 at 22-24°C. Recording from granule cells of the dentate gyrus, Edwards et al. (1990) found a rise-time smaller than 1 ms and a bi-exponential decay (2.0±0.4 ms and 54.4±18.0 ms at 21-23°C).

Spontaneous PSC conductances calculated by dividing the mean peak current by the chloride driving force is in the range 0.26-0.56 nS in CA1 pyramidal cells (Ropert et al., 1990), 0.1-2.86 nS for CA3 pyramidal cells (Hosokawa et al.., 1994), 0.49±0.42 nS (Otis and Mody, 1992) in dentate gyrus granule cells or in the range 0.2-2.0 nS according to Edwards et al. (1990).

We measured spontaneous GABAergic currents from pyramidal cells and from SL-M interneurons (fig.9). Because of the scarcity of literature on the characteristics of SL-M interneurons it was possible to make a comparison only with the data obtained from pyramidal cells. Our results show that in the CA3 (n=27) and CA1 (n=47) region sPSCs have a rise-time of 3.6±0.9 ms and 2.9±0.4 ms, respectively and a monoexponental decay with time constant 32.9±1.7 ms and 31.7±1.5, respectively. The mean

Spontaneous GABAergic activity

Pyramidal neuron

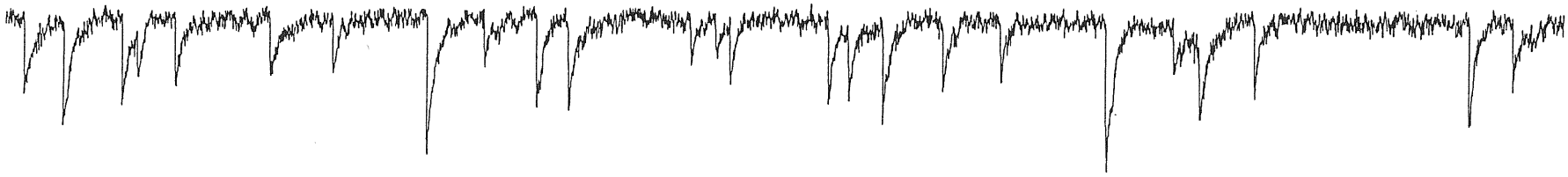

Interneuron of Stratum Lacunosum-Moleculare

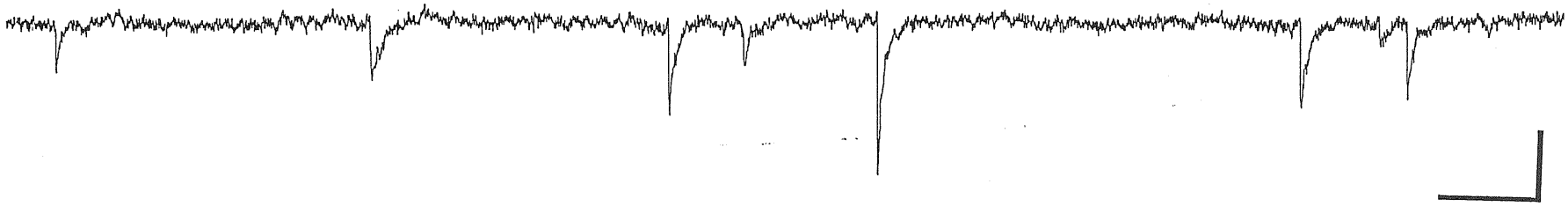

Fig. 9 Voltage clamp recording of spontaneous GABAergic activity

Both pyramidal neuron (above) and interneuron (below) display spontaneous inward currents (in the presence of glutamate receptor blockers) which are abolished by bicuculline. The kinetic characteristics of spontaneous events in pyramidal cell or in interneuron do not differ significantly.

Evoked PSCs, recorded in the presence of the glutamate-receptor blocker kynurenic acid (1mM), were abolished by 10 μM bicuculline methachloride.

conductance was 0.26±0.6 nS in CA1 and 0.46±0.07 nS in CA3. Kinetics and mean conductance are thus largely comparable with the data of Edwards et al. (1990) and Hosokawa et al. (1994).

Tab.1 Literature data reporting the characteristics of spontaneous GABAergic PSCs in the hippocampus.

GABAergic sPSCs	region	tempera-ture (°C)	mean conduc-tance (pS)	rise time (ms)	decay time (ms)
Ropert & al.	CA1	25	250-560	3.1	21-28
Hosokawa &al.	CA3	22-24	100-2860	-	29 ± 4
Edwards & al.	DG	21-23	200-2000	< 1	2.0±0.4 , 54.4±18 (bi-exp)
Otis & Mody	DG	22-24	200-400	-	21.8±2.7
Sciancalepore & al.	CA1	20-22	-	2.3±0.1	32 ± 4

3.4.2 Evoked synaptic activity

Several groups reported measurements of evoked GABAergic synaptic events. Again, comparison between data is not straightforward because of different ways of stimulation and/or different temperature of recording. Lambert and Wilson (1993) evoked GABAergic PSCs (ePSCs) stimulating Stratum Pyramidale either with a patch pipette or with a monopolar tungsten electrode in the CA3 region. At the temperature of 31°C they report a rise-time of 0.8-1.0 ms and a decay-time of 8.9-11.0 ms. Pearce (1993) evoked GABAergic PSCs in CA1 stimulating from both Stratum Pyramidale (SP) or Stratum Lacunosum-Moleculare (SL-M), and showed significant differences between SP-evoked and SL-M-evoked events with the SP-evoked ones displaying faster kinetics. Rise-time was 2.3±0.4 ms for SP-evoked and 3.8±0.9 ms for SL-M-evoked PSCs. The decays of PSCs evoked by Stratum Radiatum (SR) stimulation were fitted by the sum of two exponential functions with time constants of 4.0±0.8 ms for the fast component and 39.2±5.2 ms for the slow one at a resting potential of -80 mV. On the other hand, the decays of SP-evoked PSCs displayed only the fast component (3-8 ms). Edwards et. al (1990) recorded

from DG granule cells at room temperature stimulating the granule cell layer itself. A fast kinetic was found with a submillisecond rise-time and a bi-exponential decay with time constants 2.2±1.3 ms and 54.4±18.0 ms. Mean conductances were from 6.0±0.5 nS in CA3 (Lambert and Wilson, 1993) to 12 nS in CA1 (Pearce, 1993) or 0.14-3 nS in DG granule cells (Edwards et al.).

In the present study evoked GABAergic PSCs from SL-M (see the example in fig. 10) had an average rise time of 3.3±0.7 ms and a monoexponential decay with time constant 35.0±4.7 ms in CA1 with an average conductance of 1.28±.0.39 nS (n=11). Although kinetic parameters are comparable with those obtained by Pearce (1993) the mean conductance is sensibly smaller than that reported by Pearce (1993) and by Lambert and Wilson (1993), probably because of our choice of working with a relatively high number of failures in order to get the number of excited fibers as small as possible. The random nature of the release and the high number of failures probably is also the reason why we measured relatively large fluctuations in the ePSCs amplitude, with a variance of about 30 % of the mean response.

Tab.2 Literature data reporting the characteristics of evoked GABAergic PSCs in the hippocampus.

GABAergic ePSCs	region	tempera-ture (°C)	mean conduc-tance nS	rise time (ms)	decay time (ms)
Lambert & Wilson	CA3	31	6.0 ± 0.5	0.8-1.0	8.9-11.0
Pearce	CA1	22-24	12	3.8±0.9	4.0±0.8 , 39.2±3.2 (bi-exp)
Edwards & al.	DG	22-24	3-14	-	2.2±1.3 , 54±18

3.4.3 Miniature currents

GABAergic spontaneous events were not suppressed by the application of 1 μM tetrodotoxin (TTX). Miniature PSCs (mPSCs) were in fact still present with a frequency lower than that of sPSCs although their mean amplitude was greatly diminished. Kinetic parameters were not significantly varied by TTX application. In CA3 pyramidal cells, the frequency of sPSCs in Krebs control solution

Evoked GABAergic activity

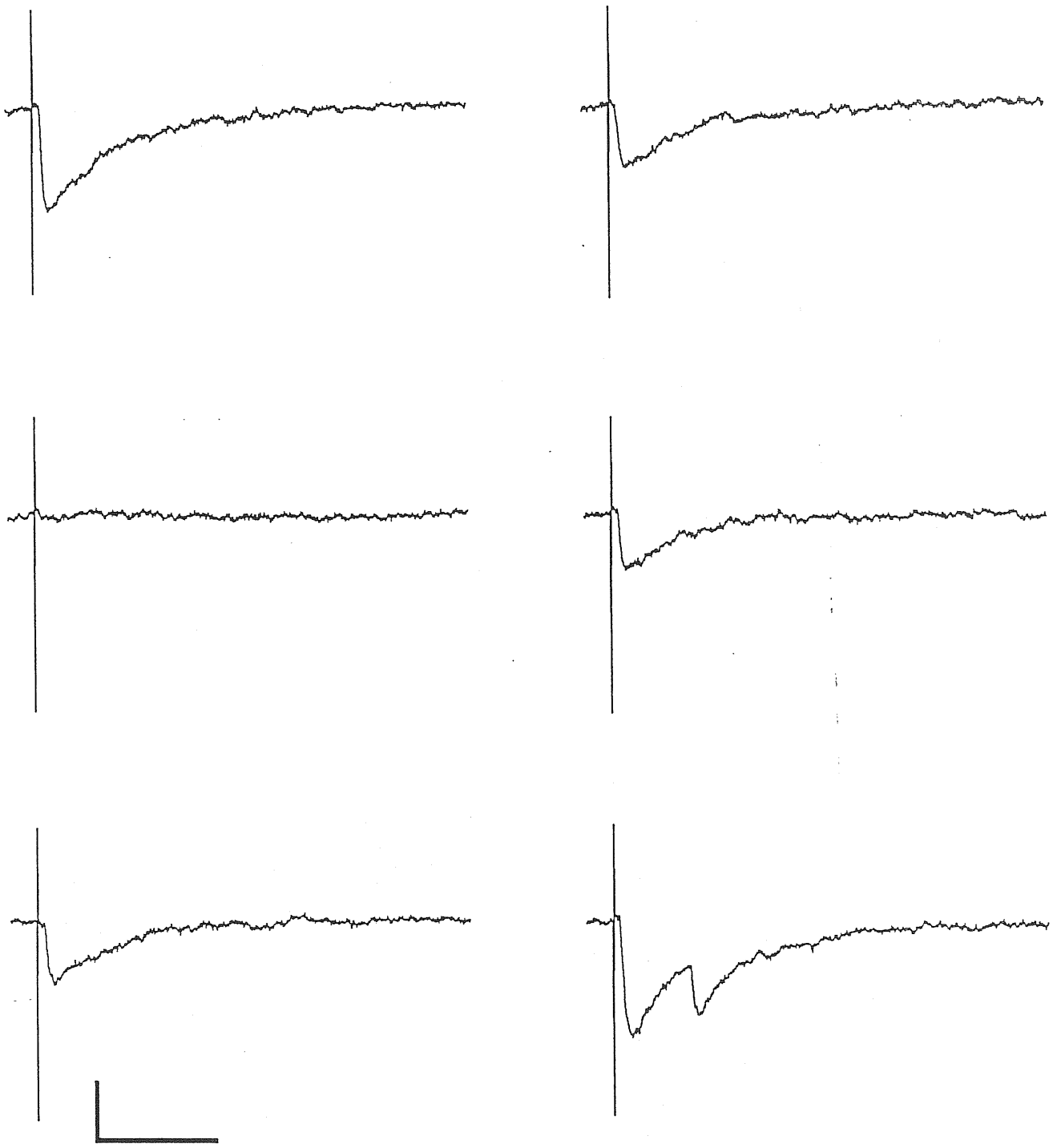

Fig. 10 Voltage clamp recording of evoked GABAergic currents

Pyramidal neuron receive a GABAergic afference from fibers activated by stimulation of Stratum Lacunosum-Moleculare. Stimulation was delivered through a patch microelectrode filled with extracellular solution. The stimulus length was 100 μs with 12 V intensity. The amplitude of the current evoked by the same stimulus is a random quantity presenting also some null event (failure). Because of the randomness of the process averages were taken usually over 50 events.

Calibration: 50 pA, 50 ms

was 0.86±0.30 Hz (n=11) while mPSC frequency was 0.25±0.04 Hz (n=5). In CA1 average miniature frequency was exactly the same (0.25±0.05, n=6).

Chapter 4

Comparison between GABAergic activity in pyramidal cells and in SL-M interneurons

4.1 General features of spontaneous synaptic activity

Because of its clear-cut borders between the Stratum Pyramidale and SL-M layer, the CA1 region was selected to perform a comparison between the spontaneous GABAergic activity in visually identified cells of these two zones. The cells were recognized as pyramidal cells or interneurons on the basis of their firing response to a current step in current clamp mode, as described above. Twentysix cells recorded from the SP layer displayed the accommodating firing pattern typical of pyramidal cells (fig.11,a left) whereas 20/24 cells recorded in the SL-M displayed the non-accommodating firing pattern characteristic of interneurons (fig.11,a right). In 4 cells patched in the SL-M current pulses did not produce a clear accommodating or non accommodating firing pattern and were thus discarded from further analysis. Pyramidal cells and SL-M interneurons had different input resistance (232 ± 32 MΩ pyramidal cell, n=24, 363 ± 92 SL-M interneurons, n=18, $p<0.05$).

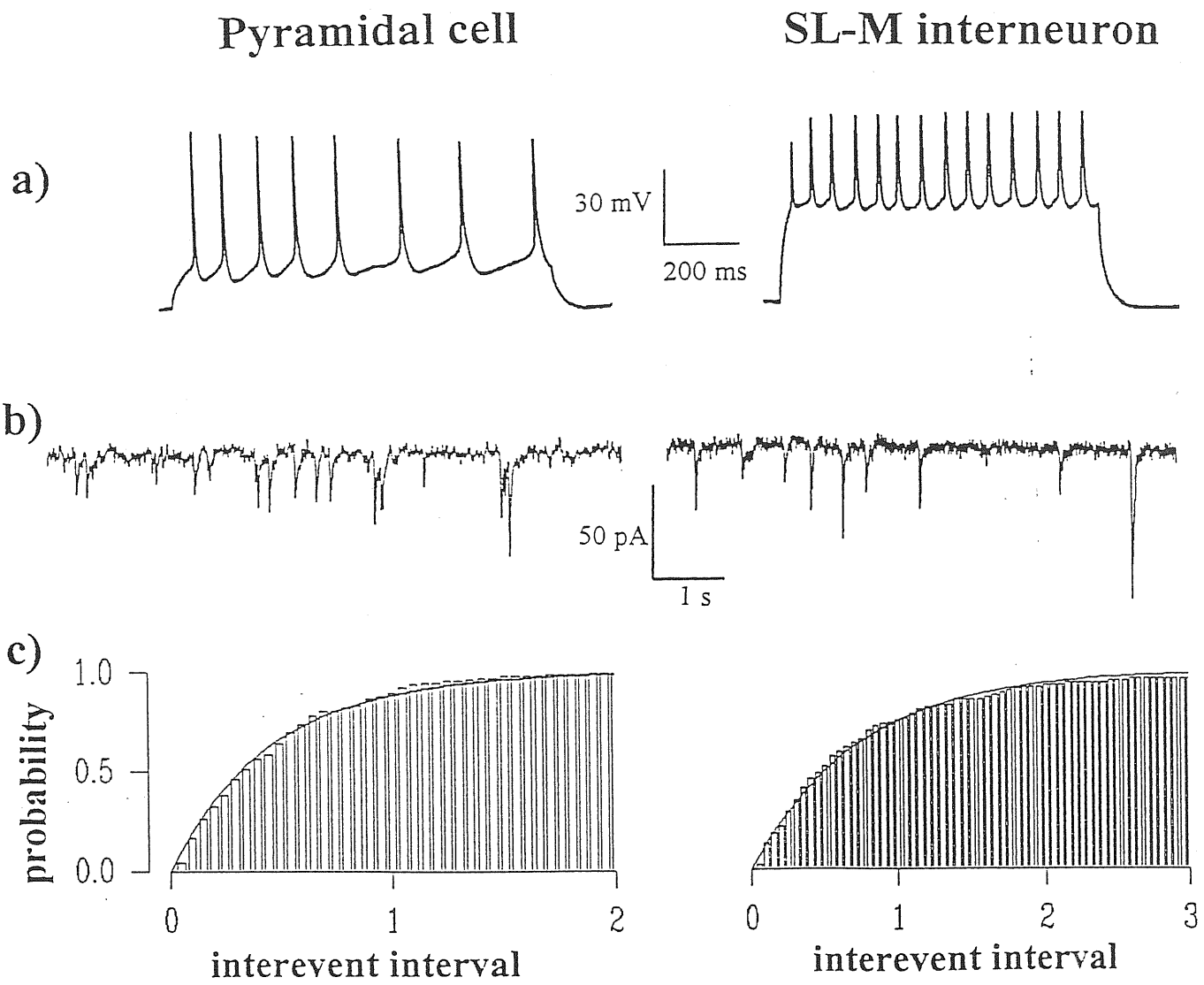
Pyramidal cell
SL-M interneuron
a)
30 mV
200 ms
b)
50 pA
1 s
c)
probability
1.0
0.5
0.0
0
1
2
interevent interval
0
1
2
3
interevent interval

Fig. 11: Comparison between properties of pyramidal cells and SL-M interneurons

a) Current clamp recording. Response to a depolarizing current pulse of 80 (pyramidal) and 50 pA (interneuron) lasting about 1 s. Membrane potential was -70 mV in both cells. Pyramidal cell and SL-M interneuron displayed respectively the typical accommodating and non-accommodating pattern.

b) Voltage clamp recording (-70 mV holding potential). In 1 mM kynurenic acid and symmetrical Cl^- concentration pyramidal cells as well as SL-M interneurons displayed spontaneous, bicuculline sensitive inward currents.

c) Cumulative interevent latency of the currents was described by an exponential curve: $A(t) = 1 - e^{-(t/\tau)}$ (solid line), where τ is the reciprocal of the mean frequency. The bin width is 50 ms for both histograms. The value of τ is 0.46±0.06 s for the pyramidal cell and 0.74±0.13 s for the SL-M interneuron.

Under voltage clamp both pyramidal cells and SL-M interneurons displayed sustained, spontaneous, synaptic activity (see fig.11,b). Spontaneous PSCs were abolished by 2 μM bicuculline methiodide, or 50 μM picrotoxin, or 2 mM penicillin G, and their reversal potential was about 0 mV, close to the Nernst potential for chloride in SL-M interneurons as well as in pyramidal neurons. Applications of bicuculline elicited a significant variation of the baseline current (7.0 ± 2.6 pA, n=6, $p<0.05$) towards more negative values. Application of TTX decreased the frequency of sPSCs recorded from SL-M interneurons by 88±32% (n=3). Mean frequency, amplitude, rise-time and decay-time of sPSCs in pyramidal cells and SL-M interneurons in control conditions are reported in Tab.3 .

Tab. 3: comparison between kinetic characteristics of GABAergic synaptic currents in pyramidal cells or in SL-M interneurons.

mean ± s.e.m.	pyramidal cells CA3	n	pyramidal cells CA1	n	SL-M inter-neurons CA1	n
frequency (Hz)	0.86 ± 0.30	27	0.75 ± 0.26	26	0.53 ± 0.11	20
amplitude (pA)	18.1 ± 4.7	27	34.6 ± 5.0	21	39.6 ± 4.1	14
conductance (pS)	259 ± 68	27	494 ± 71	21	565 ± 59	14
rise time (ms)	3.6 ± 0.9	27	2.9 ± 0.4	8	3.2 ± 0.3	13
decay time (ms)	32.9 ± 1.7	27	31.7 ± 1.5	8	32.3 ± 2.4	13

Sampling rate was 4 kHz. No variations were detected in any of the parameters using non-paired *t*-Student test at 5% of significance.

None of them was significantly different between pyramidal cells and interneurons. Analysis of the interevent interval distribution was performed on 5 pyramidal cells and on 5 SL-M INs. To eliminate the dependency on the bin size, histograms of cumulative interevent interval were calculated as

shown in fig. 11 b) for a PC (left) and a SL-M IN (right). In all cases it was possible to represent the histogram with a function

$$A(\Delta t) = [1 - e^{-(\Delta t/\tau)}] \quad ,$$

as shown in the example of fig.11 c (continuous lines) where Δt is the event interval and τ is the inverse of the mean frequency, for PCs as well as for SL-M INs. This description is equivalent to the distribution of interevent intervals by a 0-order poissonian with time constant τ.

4.2 Modulation of sPSCs frequency

Various drugs agonists were used to reveal possible differential modulation of sPSCs from CA1 pyramidal cells or interneurons. Among those tested the most effective in changing sPSCs frequency were furosemide, carbachol, trans-1-aminocyclopentane-1,3-dicarboxilic acid (t-ACPD), l-Arg, baclofen and serotonin (5-HT). Furosemide blocks the membrane Cl^--cation transporter (Misgeld et al., 1986, Thompson and Gahwiler, 1989). It was used also for performing preliminary tests concerning the influence of $[Cl^-]_i$ on GABAergic interneurons, problem that was addressed in detail in chapter 6. Carbachol, t-ACPD and baclofen activate metabotropic receptors for acetylcoline, glutamate, GABA respectively in rat hippocampus (Bianchi and Wong 1994, Gerber and Gawhiler 1994, Sciancalepore et al. 1995). L-arg increases transmitter release by enhancing the synthesis of nitric-oxide (Lonart et al., 1992; Segovia et al., 1994). 5-HT affects membrane excitability through several receptors (Andrade and Nicoll 1987, Freund et al. 1990). Drugs were bath applied to the preparation in different experiments producing variations in sPSCs frequency with a time lag variable from 30 to 180 s. Furosemide (1 mM), carbachol (10 μM), t-ACPD (10 μM) and l-arg (2

mM) significantly enhanced sPSCs frequency whereas 5-HT (10 μM) and baclofen (10 μM) produced the opposite effect, regardless the cell type from which sPSCs were recorded (fig.12 1-6). The results are reported in tab.4 as percentage of frequency variation after pharmacological treatment.

Tab. 4: Increase in PSC frequency in CA1 pyramidal cell or in SL-M interneurons after pharmacological treatment.

frequency variation (%) after treatment	pyramidal cells	n	SL-M interneurons	n
1 mM furosemide	+ 65 ± 41	4	+ 151 ± 68	4
10 μM carbachol	+309 ± 118	5	+257 ± 70	5
10 μM t-ACPD	+160 ± 100	*	+371 ± 179	4
2 mM L-arg	+ 57 ± 29	3	+ 142 ± 31	4
10 μM 5-HT	- 57 ± 30	3	- 44 ± 29	3
10 μM baclofen	- 97 ± 22	3	- 94 ± 34	3

The percentage of variation in sPSC frequency was calculated from the samples indicated. Bath-applied furosemide, carbachol, t-ACPD and L-arg increase sPSC frequency whereas 5-HT and baclofen reduce frequency in CA1 pyramidal cells as well as in SL-M interneurons. Statistical significance within each group is assessed with the paired *t*-Student test. The asterisk (*) indicates data taken from Sciancalepore et al. (1995).

Postsynaptic effects were also present. Input resistance was varied by carbachol (+32±18% in PCs, n=5, and +33±5% in SL-M INs, n=5), 5HT (-80±55% in PCs, n=3 and -60±37% in SL-M INs, n=3) and baclofen (-25±4% in PCs, n=3 and -20±6 in SL-M INs, n=3) while it was unchanged by t-ACPD.

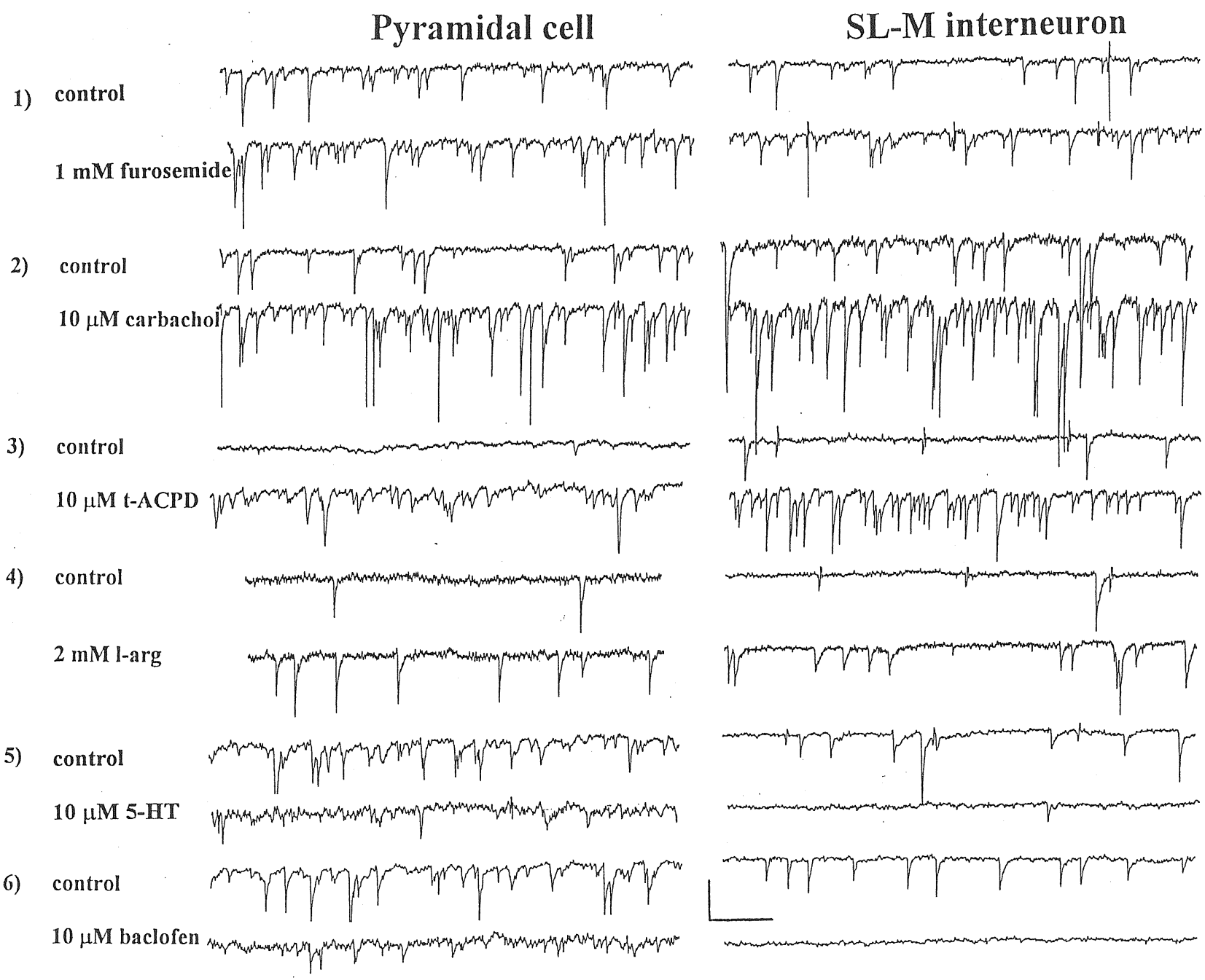
Pyramidal cell
SL-M interneuron
1) control
1 mM furosemide
2) control
10 μM carbachol
3) control
10 μM t-ACPD
4) control
2 mM l-arg
5) control
10 μM 5-HT
6) control
10 μM baclofen

Fig. 12: effect of different drugs on sPSC frequency

Voltage clamp recording of sPSCs frompyramidalcells (left) and SL-M interneurons (right). In each pair of traces the upper one was recorded in control conditions and lower one starts 30-150 s after pharmacological treatment. Furosemide (1 mM), carbachol (10 μM), t-ACPD (10 μM) and l-arg (1mM) increase the frequency of sPSCs whereas 5-HT (10 μM) and baclofen (10 μM) decrease sPSC frequency in pyramidal cells as well as in SL-M cells. Calibration bar 1 s, 20 pA.

4.3 Simultaneous recording from a pyramidal cell and SL-M INs.

GABAergic neurons producing sPSCs could in principle establish synapses with different cell types. To address the question whether a same GABAergic cell eliciting sPSCs on a PC could contact a neighbour SL-M IN, simultaneous patch-clamp recording of sPSCs was performed on PC - SL-M IN pairs. The presence in the two traces of correlated sPSCs would indicate a common afference. A distance of about 150-200 μm separated pyramidal cell and interneuron in each pair. Cross-correlation analysis in a window of 50 ms was performed determining the latencies between the events in one channel with respect to the events in the other one. For 3 pairs the latencies were later recalculated on the same traces displaced by 500 ms as control. The results are shown in latency histograms for the simultaneous and for the displaced traces. In fig. 13 a series of double-recorded traces are shown (left) with the related correlogram (right). Higher time resolution of simultaneous events is shown in fig. 14. Cross correlation was established when histograms from simultaneous traces displayed a clear peak around the origin. The latency histogram evaluated for the same traces displaced by 500 ms did not display any clear peak (n=3). A further control parameter was the frequency of randomly expected coincidences, given by $\nu_{random} = \Delta t \cdot \nu_1 \cdot \nu_2$, where Δt is the maximum accepted latency for two correlated events, ν_1 and ν_2 are the sPSCs frequencies in the two cells. Two events were considered as coincident if they showed a latency difference $|\Delta t| \leq 4$ ms. Using 4 ms as bin width, on 10/12 pyramidal-interneuron pairs, a clear peak in the histogram of simultaneous traces was present, indicating the presence of a simultaneous input. In 10/12 cells the average frequency of the simultaneous events (0.088±0.041 Hz) was significantly larger than the background frequency in the simultaneous traces themselves (0.021±0.010 Hz, n=10, $p<0.05$), the frequency of "simultaneous" events in the traces displaced by 500 ms (0.020±0.010 Hz, n=3, $p<0.05$), and finally the theoretically calculated frequency (0.017±0.014 Hz, n=10, $n<0.05$). The

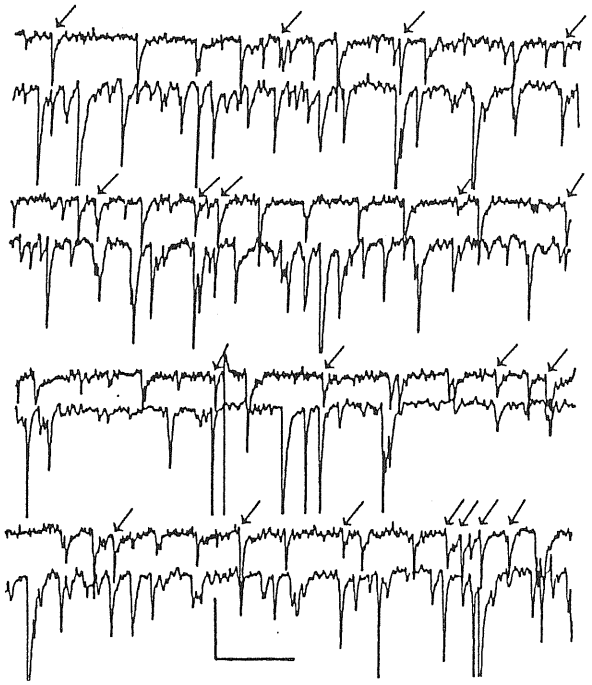

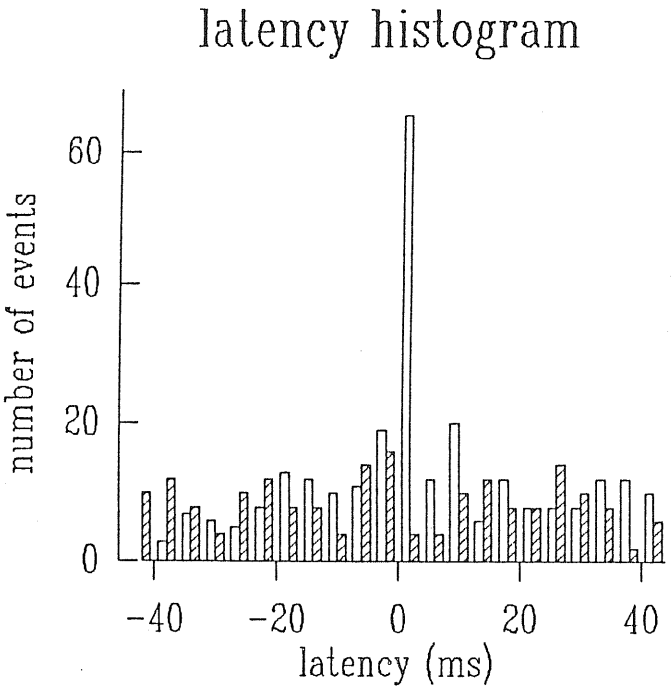
latency histogram
number of events
60
40
20
0
−40
−20
0
20
40
latency (ms)

Fig.13: double whole-cell patch-clamp recording

Left: four representative records of two-electrode patch-recording from a pyramidal cell and a SL-M interneuron (upper and lower traces of each pair). The arrows indicate pairs of events at a time lag (t) $\leq$ 4 ms. Calibration bar 1 s, 100 pA. Right: latency histogram of the two cells. The number of events at a given latency from each other was evaluated over a 500 s long record sampled at 1 kHz. The bin width was 4 ms. The histogram with striped bars was calculated shifting the traces by 500 ms, open bars represent the histogram from the simultaneous traces. The amplitude of the correlated events at 0 ms latency is about 6-fold the average amplitude at the other latencies.

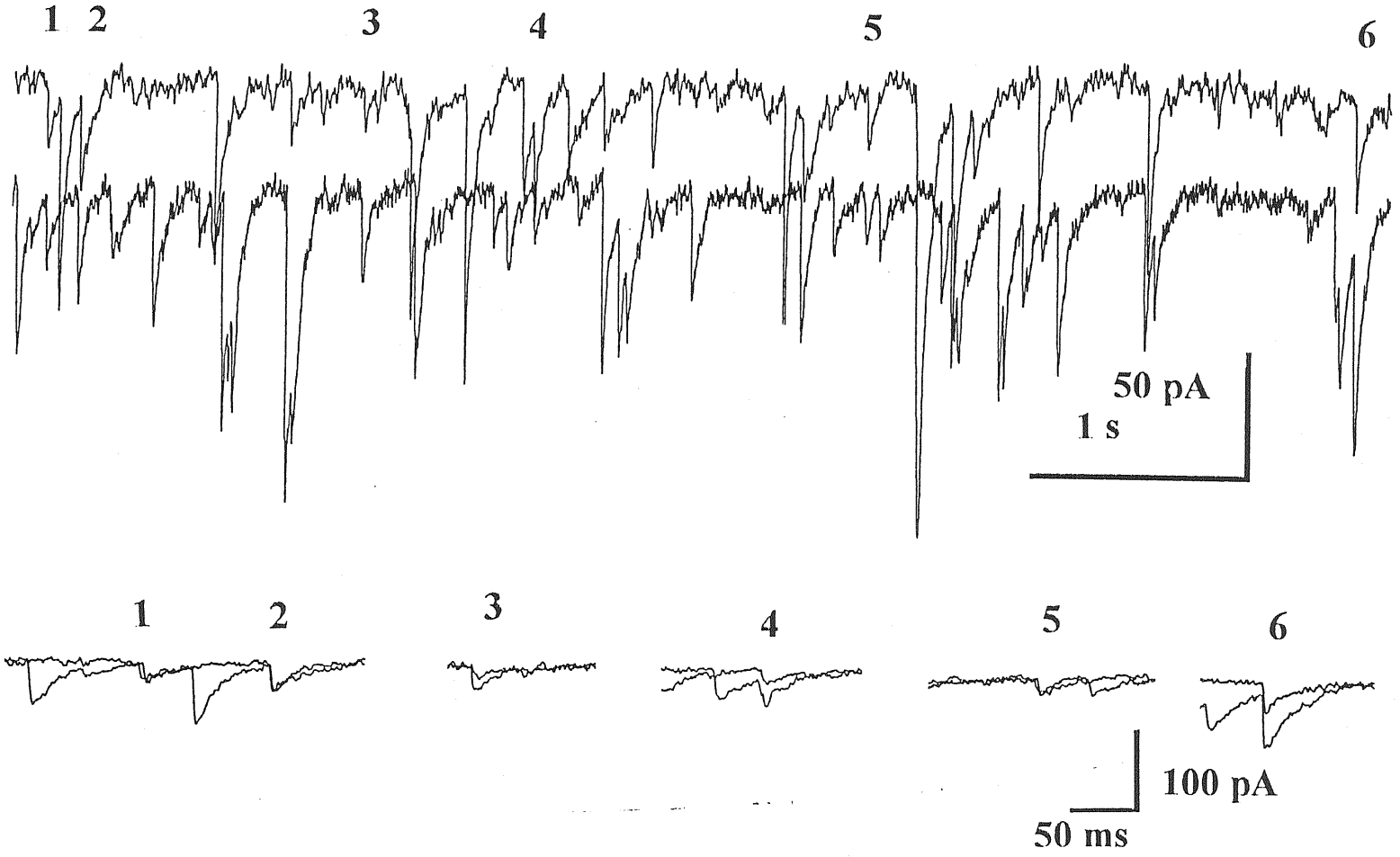
1
2
3
4
5
6
50 pA
1 s
1
2
3
4
5
6
100 pA
50 ms

Fig. 14 double-patch recordings

Simultaneous events shown on an expanded scale. Only accurate analysis in the millisecond range can assess real simultaneity of the GABergic events.

number of detected coincidences was thus on average 4-5 times larger then the number of randomly expected ones. In 2 cases carbachol was applied to increase sPSCs frequency. The ratio between measured and randomly expected coincidences ($\nu_{measured}/\nu_{random}$) was not significantly changed by the treatment ($\nu_{measured}/\nu_{random}$ = 6.2±1.3 in control conditions and 5.8±2.8 after treatment). An analysis of the delays between the correlated events was also performed. Considering the pairs of events in each of the two channels that occurred at latencies shorter than 4 ms, the average difference in the latencies (0.70±0.91 ms, n=10) did not significantly deviate from 0, indicating that in the paired events none of them significantly preceded or followed the correlated one.

Chapter 5

Modulation of GABAergic activity by TRH

Another set of experiments was performed to test the effects of TRH. A high concentration of TRH-receptor has been found in the CA1 region of the hippocampus (Sharif, 1989). This region was therefore selected for testing the effect of the hormone on spontaneous and evoked GABAergic PSCs. In this case the intracellular solution Intra2 was used, which allowed to discern pyramidal neurons from interneurons after examination of their firing pattern.

5.1 Spontaneous activity

5.1.1 Pyramidal cells

Spontaneous sPSCs were present in all recorded pyramidal cells, identified by visual inspection. These cells displayed a typically accommodating firing pattern (see fig.15,a). Applications of 10 μM TRH

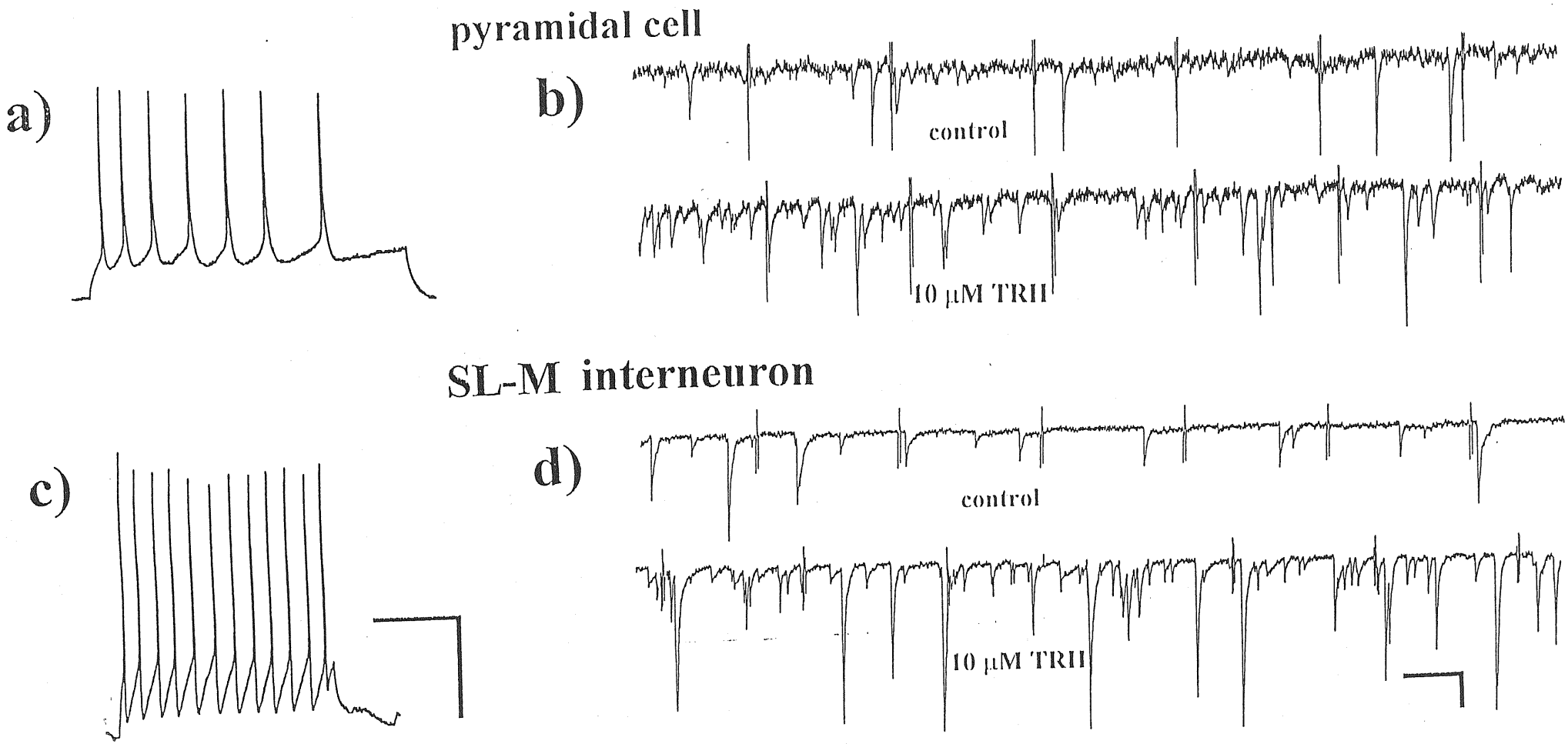
pyramidal cell
a)
b)
control
10 μM TRH
SL-M interneuron
c)
d)
control
10 μM TRH

Fig. 15 Effect of TRH on sPSCs

Patch-clamp recording was performed from visually identified pyramidal neurons or from interneurons of SL-M layer. a) and c) are current clamp responses to a 40 pA current pulse (0.8-1 s). The pyramidal cell displays typical accommodating firing pattern while the interneuron supports regular, high frequency spiking with virtually no accommodation. Calibration bars: 400 ms, 50 mV. Spontaneous PSCs recorded, under voltage clamp, from pyramidal cell (b) as well as from SL-M interneuron (d) are shown as downward deflections (inward currents) and are sensitive to TRH application. Note that tracings also contain outward (upwards) current responses (plus transients) elicited by 5 mV step pulses (40 ms) used to regularly monitor cell input resistance. In each pair of traces (b and D) upper records are controls while lower ones are after two min application of TRH (10 mM). Kynurenic acid (1mM) is present throughout to eliminate the glutamatergic drive. The increase in frequency is from 1.9 Hz to 6.1 for the pyramidal cell and from 1.8 to 8.0 for the SL-M interneuron. Mean sPSC amplitude is not significantly varied by TRH. Calibration bars: 1 s, 20 pA.

elicited (after 30-60 s) an enhancement in the frequency of sPSCs in 21/24 CA1 pyramidal cells as shown by the sample tracings in fig.15,b. The phenomenon of enhanced frequency of sPSCs usually outlasted the 2-3 min application of TRH with a gradual return to baseline values after approximately 20 min. When the application of TRH was repeated at this time, no response was observed. However, TRH application after further 30 min wash elicited a response virtually identical to the first one. Therefore, an interval of at least 30 min was regarded as the minimum recovery time between successive applications. Because of such a long-lasting desensitization to the action of TRH it was not possible to perform a dose-frequency response curve. In 3 cells TRH was continuously superfused for 20 min. In these cases the rise in frequency peaked at about 60 s and lasted for 8-15 minutes, followed by a gradual decline in frequency and amplitude of the sPSCs. Thirty-min washout was sufficient for substantial recovery. On average, after application of TRH, the frequency of sPSCs increased from 1.07±0.68 Hz to 3.16±0.73 Hz ($p<0.01$, $n=21$) as evaluated from records starting one to two min after the drug application. Fig.16 is an exemple of frequency variation after TRH application as shown by the cumulative distribution of the interevent interval. In the majority of cells (16/21) TRH did not significantly change the amplitude of sPSCs (29.4±7.6 pA in control vs. 33.7±12.1 pA in TRH); on a sample of 21 cells only in 5/21 cells the amplitude was significantly increased (108±13 %, see fig.17) after 3 min application of TRH as shown in the example of fig.18 (upper panel) in which while the mean sPSCs amplitude almost doubles the other kinetic parameters (rise- and decay-time) remain unchanged (Fig.18, middle and bottom panels). Cell input resistance did not vary in the presence of TRH (133±34 MΩ in control vs. 125±45 MΩ in TRH, n=24). Even when the input resistance was examined for the subset of 5 neurons upon which TRH elicited an increased amplitude of sPSCs, no significant change was found (-10±14%), which ruled out that the increase in postsynaptic currents was due to enhanced membrane resistance. TRH application did not significantly change sPSC mean decay-time (39.7±12.8 ms in control vs. 35.2±4.4 ms in TRH, n=9) or rise-time (3.2±0.5 ms in control vs. 2.9±0.5 ms in TRH, n=11). In order to check for a possible direct regulation by TRH of GABA release mechanisms, miniature PSCs (mPSCs) were recorded after block of

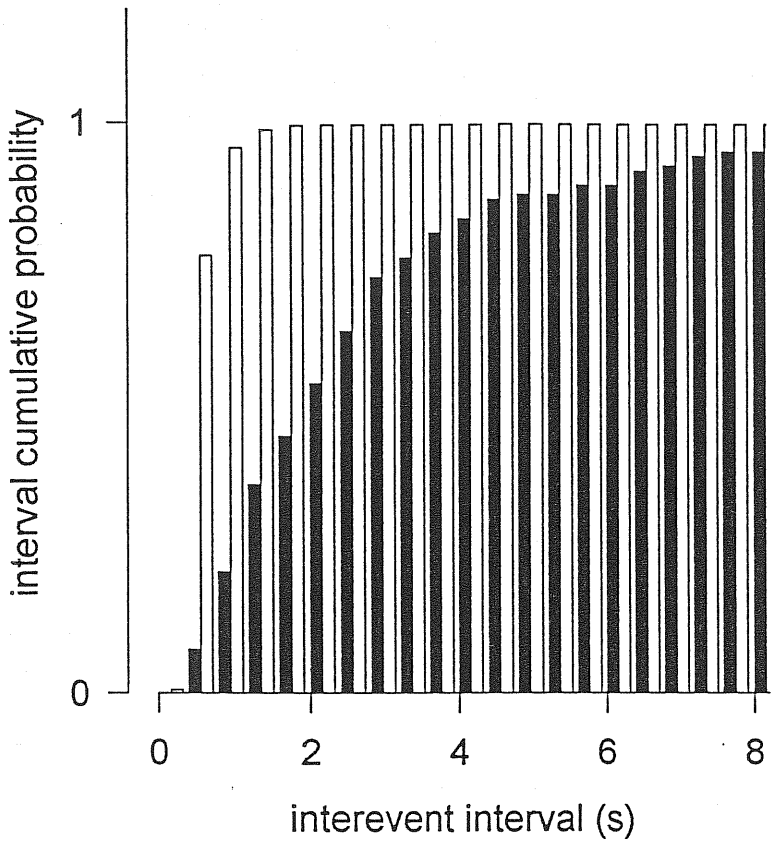
interval cumulative probability
1
0
0
2
4
6
8
interevent interval (s)

Fig. 16 Rise in frequency after TRH application

Cumulative probability histogram of the interval between adjacent sPSCs in control (filled bars) or after 10 μM TRH (open bars). The mean interevent interval decreases from 2.5 ± 0.2 to 0.6 ± 0.3 s in TRH corresponding to an increase in the frequency of sPSCs of 1.27 Hz.

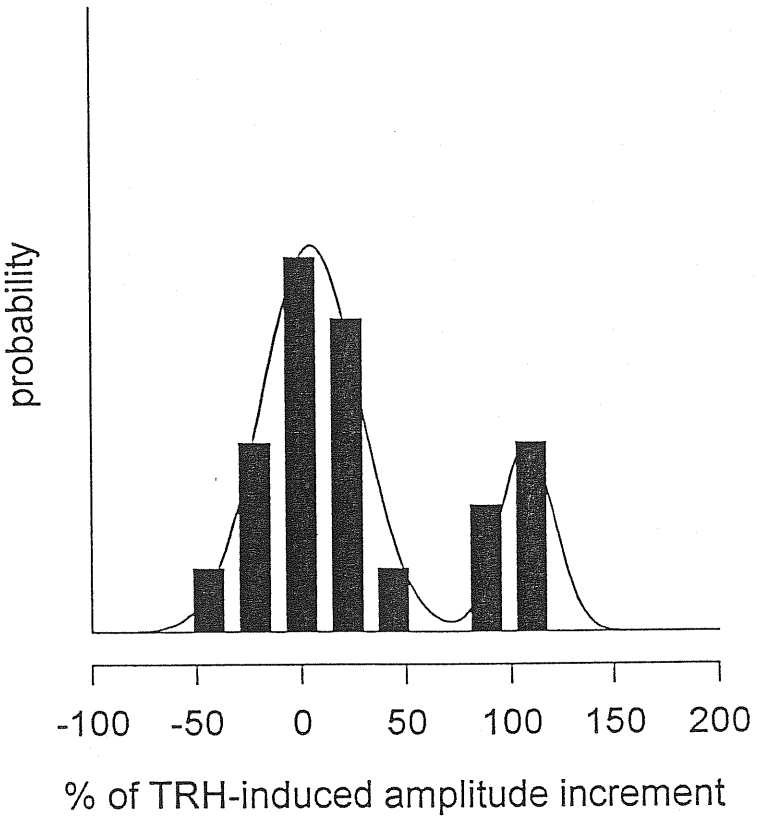
probability
-100
-50
0
50
100
150
200
% of TRH-induced amplitude increment

Fig.17 effect of TRH on sPSC mean amplitude

Histogram of the mean amplitude variation (%) in TRH rispect to the control. On a sample of 21 cells a population is clear in which the amplitude is unvaried by TRH whereas for a minority of cells (5/21) the mean amplitude approximately doubles its amplitudes. The continuous line represents the fit of the distribution with the sum of two gaussians.

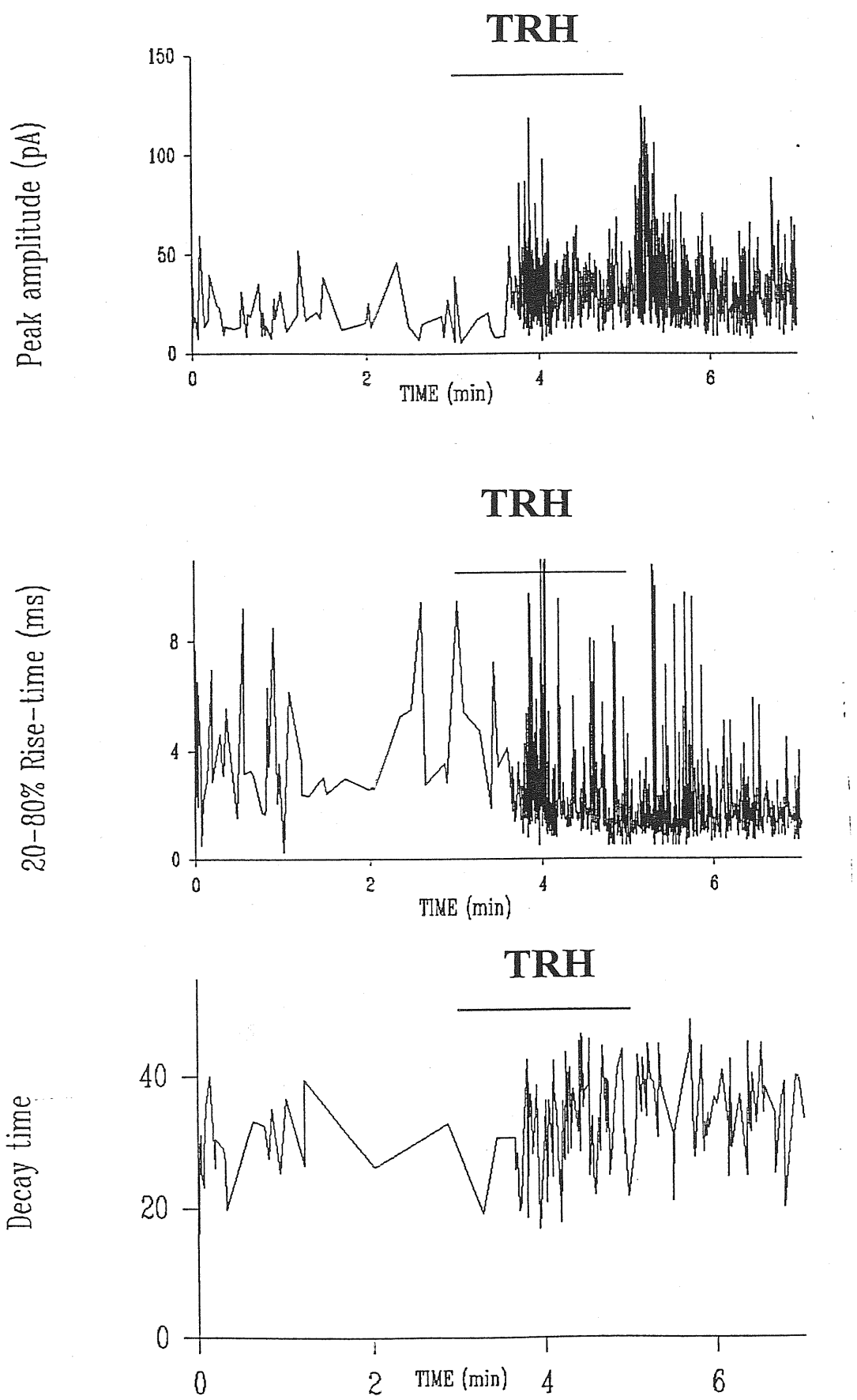

Timecourse of the action of 10 μM TRH

Fig. 18 Timecourse of TRH effect on GABAergic sPSCs

Amplitude (upper panel), rise-time (middle panel) and decay-time (lower panel) of sPSCs before and during the action of 10 μM TRH, indicated by the horizontal bar are shown. In spite of the marked increase in frequency none of these parameters was significantly changed. Rise-time and decay-times were calculated only for a subset of the total events.

action potentials by TTX (1 μM). Application of TRH in TTX solution did not significantly affect mPSC frequency (0.25±0.05 Hz in control vs. 0.23±0.05 Hz in TRH, n=6).

5.1.2 Localization of cell responsiveness

To identify the regional location of TRH-sensitive GABAergic neurons mini-slices were cut from transverse hippocampal slices by removing the dentate gyrus, the CA3 area or both, as shown in fig.19.

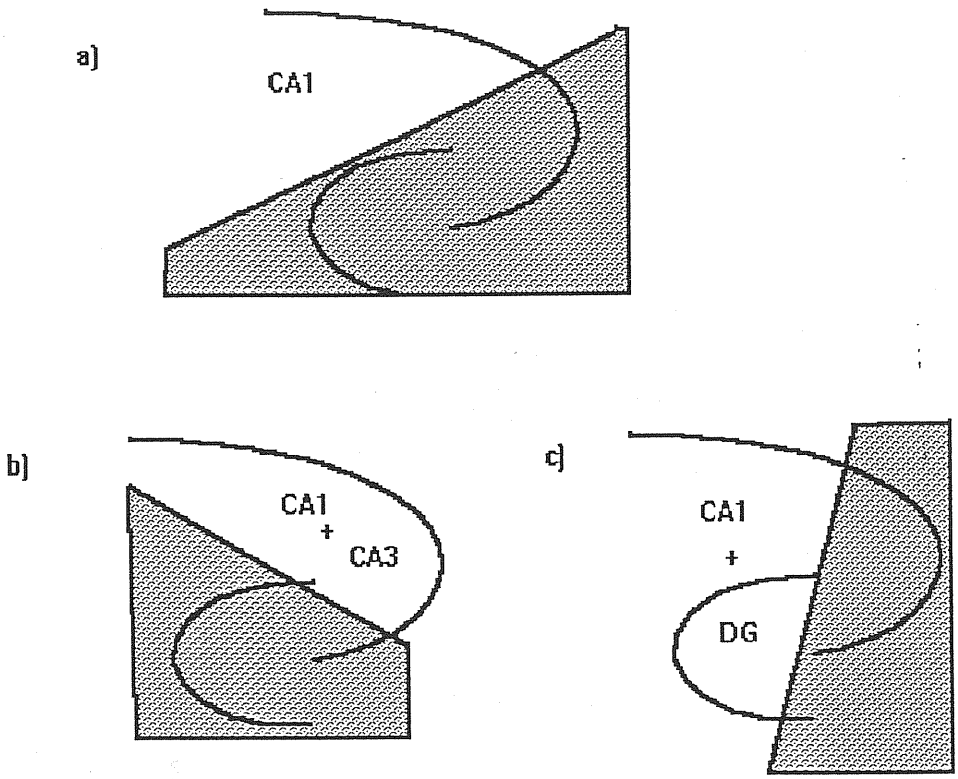

Fig. 19 Hippocampal thin slices were cut further in order to remove regions as indicated by shaded areas.

7/8 cells displayed sPSCs in control or after the application of 10 μM TRH and in all cases TRH enhanced sPSC frequency. Assigning the numbers I, II and III to the groups lacking respectively CA3, dentate gyrus and both, the increase in frequency was from 3.49 Hz to 5.98 Hz for group I (n=3), from 1.12 Hz to 2.65 Hz for group II (n=2) and from 0.57 Hz to 3.36 Hz for group III (n=3). The variation of the frequency for

the the whole group was from 1.56±0.95 Hz in control to 3.76±1.22 Hz after TRH. The variation in frequency for the whole set and for group III were statistically significant ($p<0.05$).

5.1.3 Interneurons of SL-M

Interneurons were identified in SL-M and patch-clamped using the same conditions as for pyramidal cells. The presence (or absence) of accommodation in the firing pattern (in current clamp mode) provided a functional identification of the cell type (fig. 15,c). Mean amplitude (23.8±5.7 pA), rise-time (3.2±0.5 ms) and decay-time (42.7±4.8 ms) of sPSCs were not significantly different from those recorded from pyramidal cells (n=6). Application of 10 μM TRH elicited also in this case an increase in sPSC frequency from 1.63±0.61 Hz to 3.28±0.63 Hz (n=13) as shown in the example of fig. 15,d. Cell input resistance in control solution (436±159 MΩ, n=6) was significantly different ($p<0.02$) from that of pyramidal cells and was not affected by TRH application (+8±27%).

5.1.4 Simultaneous recording from a pyramidal cell and a SL-M interneuron.

In 6 cases TRH was applied during simultaneous double recording from a visually identified pyramidal neuron and a neighbouring interneuron.

The calculated frequency of random concurrences was 0.022±0.012 Hz, while the experimentally observed frequency was an order of magnitude larger, namely 0.103±0.089 (n=6). Spontaneous PSC frequency for both cell types was largely increased by TRH application (1.87±0.35 Hz in control vs. 4.31±0.72 Hz in TRH for pyramidal cells, and 1.67±0.32 Hz in control vs. 3.21±0.39 Hz in TRH for interneurons) as also found with individual cell recording. The ratio between the frequency of measured and random concurrences was 4.32±1.36 in control solution, a value virtually equal to that observed in TRH solution (4.49±0.95). This finding indicates that in the presence of TRH the strong degree of coupling of GABAergic events between the two neurons in the pair was preserved.

5.1.5 TRH induced rhythmic PSCs

In 3/25 interneurons and in 1/42 pyramidal cells TRH application induced large-amplitude PSCs regularly time-spaced at about 2 Hz as in the example in fig.19 a. Such PSCs displayed the typical kinetic and pharmacological profile of GABAergic events since they were blocked by 10 μM bicuculline and their rise- and decay-time were not significantly different from control ones. Autocorrelation analysis was performed on series of rhythmic sPSCs, considering each event as a point-like Dirac delta function $A \cdot \delta(t-t_0)$ where t_0 is its starting point, having an area equal to the event peak amplitude A. The intervals between each PSC and its next 10 adjacent events were calculated and histogrammed in each trace. A peak at about 500 ms in the autocorrelation function corresponding to the first harmonic was fitted by a gaussian curve plus a constant describing the randomly occurring intervals, as exemplified in fig. 19 b. The center of the gaussian was at 526±96 ms with a variance of 65±8 ms (n=4), corresponding to a frequency of 1.90±0.21 Hz. The ratio between the amplitude of the gaussian and the constant was 4.39±1.10, significantly different from 0 ($p<0.03$). In one case rhythmic PSCs were detected in a SL-M interneuron during a simultaneous recording from a pyramidal cell. In the pyramidal cell no large-amplitude events were readily recognizable synchronous with those in the interneuron. In one case TRH elicited large amplitude, biphasic, inward currents with kinetic characteristics different from GABAergic potentials (see. fig. 20). These currents had frequency comparable with those of GABAergic oscillations and gradually faded in about 7-8 min.

5.2 Evoked synaptic activity

In order to detect any influence of TRH on the phasic release of GABA PSCs were evoked by direct electrical activation of the local GABAergic circuitry. The stimulating electrode was placed onto the cell body of a visually identified neuron of SL-M. Focal stimulation (5-50 V; 50-200 μs) of SL-M with a patch

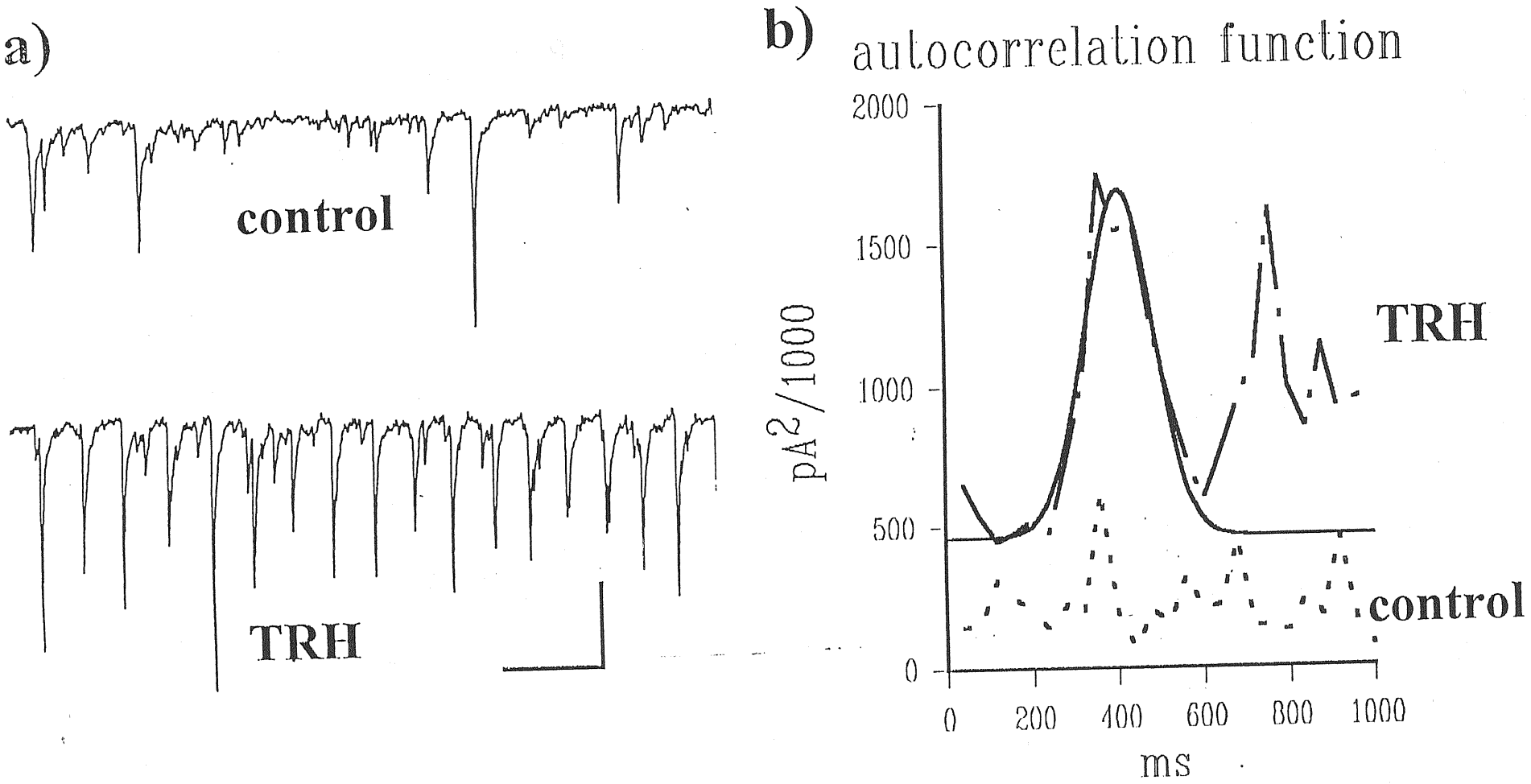
a)
control
TRH
b)
autocorrelation function
2000
1500
1000
500
0
pA²/1000
TRH
control
0
200
400
600
800
1000
ms

Fig.19 TRH induces rhythmic GABAergic PSCs recorded from a SL-M interneuron in the presence of kynurenic acid (1 mM).

a): spontaneous activity in control solution (top) and after about 2 min TRH application (bottom) when large PSCs appear in a rhythmic fashion. Calibration bars: 1 s; 5 pA. b): plot of the autocorrelation function in control (dotted line) and after application of TRH (broken line). The first harmonic of the autocorrelation function in the presence of TRH is fitted by a gaussian (continuous line) centered at 408±6 ms with 80±9 ms variance. The ratio between the amplitude of the gaussian and the baseline level is 2.66±0.18.

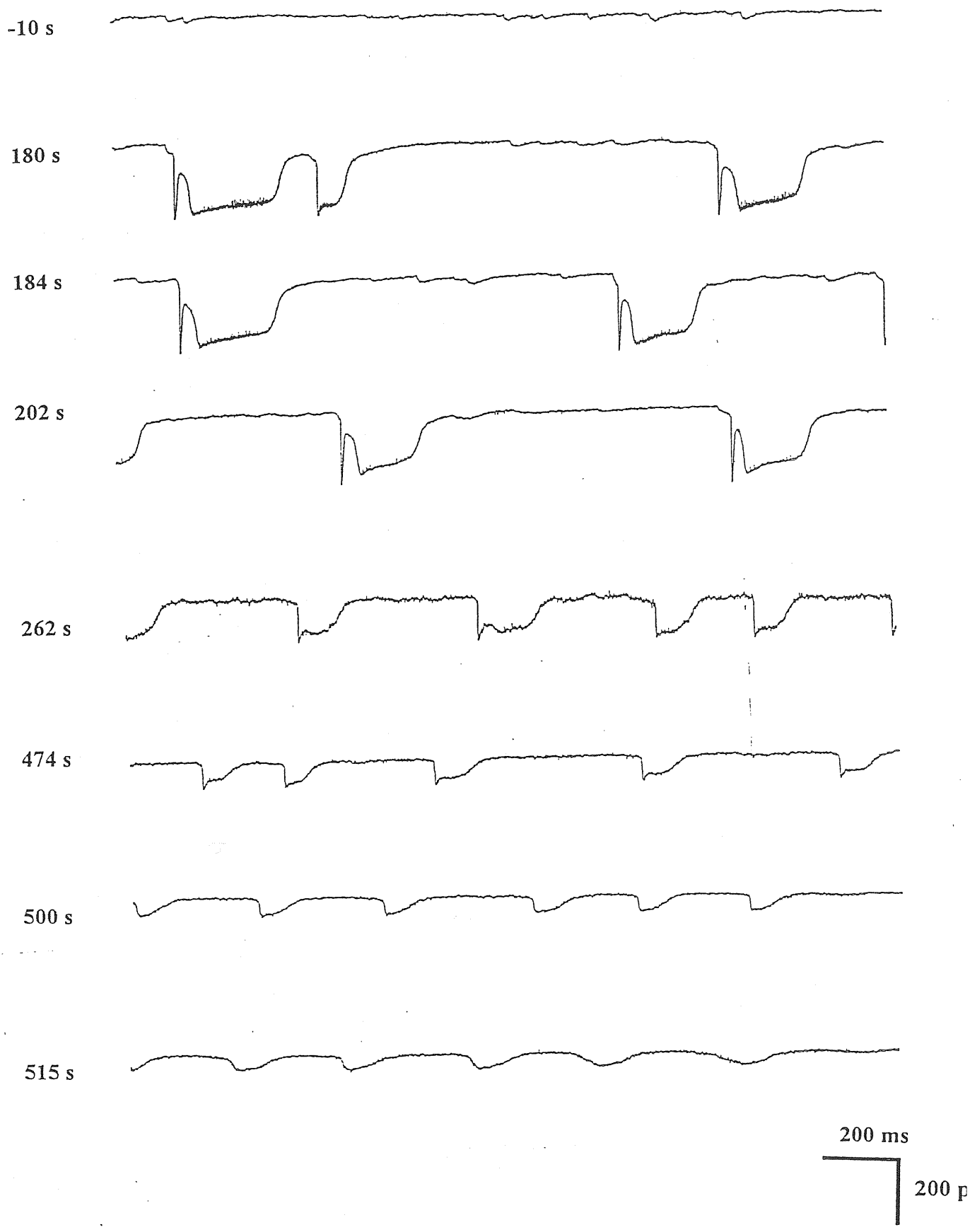
-10 s
180 s
184 s
202 s
262 s
474 s
500 s
515 s
200 ms
200 p

Fig.20 TRH-induced oscillations

Application of TRH (10 μM) elicited in a single cell wide amplitude oscillations at time lags compatible with those of the rhythmic GABAergic large-amplitude events (compare with the previous figure). GABAergic sPSCs are visible as the small deflections from the baseline. The numbers reported at the left of the traces indicates the distance of the starting point in respect to the application of TRH. The single events appear to be made up of a first rapid rising and decaying phase followed by an inward current large more than 200 ms that progressively decays in amplitude and in width but not in frequency. TRH was applied since the time 0 throughout the whole experiment.

electrode evoked PSCs at a fixed latency in the range 3-6 ms (mean latency was 4.9±0.7 ms), suggestive of a monosynaptic event as shown in the example of fig.21. Stimulation at a rate of 0.1 Hz did not induced considerable synaptic fatigue as judged by the stability of ePSC amplitude averaged over 4-8 responses. In 11 cells the application of TRH elicited a statistically significant decrease in the PSC mean amplitude from 90±27 to 44±15 pA ($p<0.05$, n=11) as shown in the example of fig.21 and 22 a,b. After elimination of the failures from the calculation, the difference in PSC amplitude was, however, no longer statistically significant (122±47 pA in control vs.82±26 pA in TRH, n=11). Rise-time (3.3±0.7 ms in control vs 3.8±1.0 in TRH, n=6) and decay-time (35.0±4.7 ms in control vs 33.1±3.1 ms in TRH, n=6) were also unchanged. TRH increased the probability of failure from 27±8% to 41±10% ($p<0.05$, n=11). An example of this effect is shown in fig.22 c,d, in which the mean of all responses including failures (displayed in c) is clearly larger in control (left) than in TRH solution (right). Conversely, after eliminating failures from the calculation, the mean amplitude of response did not decrease after TRH application (see fig.22 d).

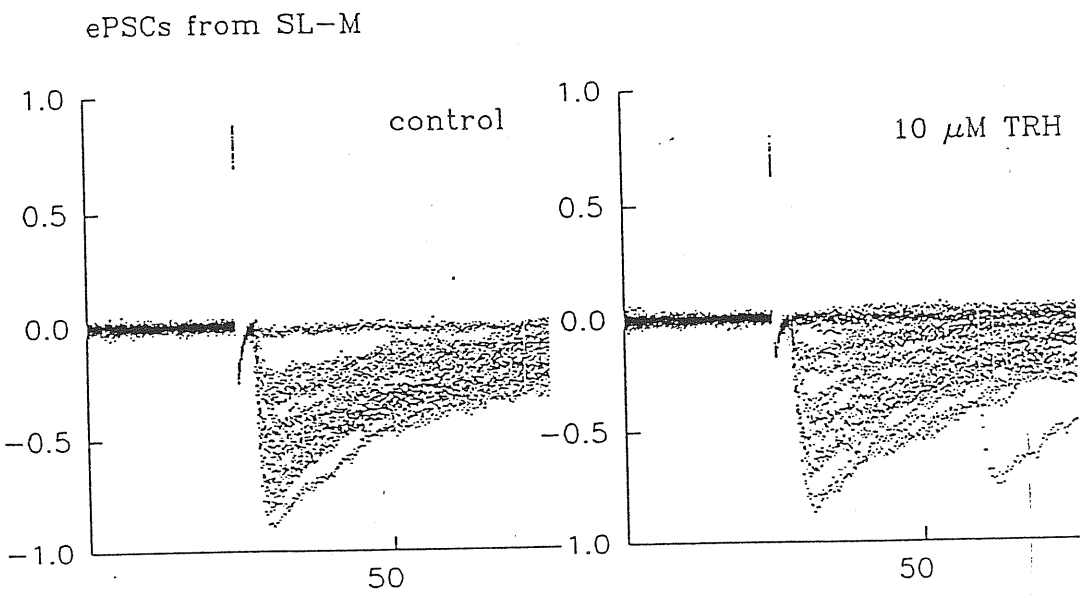
ePSCs from SL–M
control
10 μM TRH
1.0
0.5
0.0
−0.5
−1.0
50

Fig.21 TRH effect of TRH on ePSCs

Evoked PSCs are recorded from a pyramidal cell following stimulation of the SL-M layer with a patch electrode filled with extracellular solution.The first 20 of 50 evoked potentials are plotted in control (left) or after 10 μM TRH application. Stimulus intensity was 18V per 120 μs width. TRH increases the number of the failures of ePSCs from 8/50 to 16/50 leaving unchanged the amplitude of the non-failure events (0.48 ± 0.18 nA in control vs. 0.51 ± 0.21 nA in TRH). Calibrations: nA, ms.

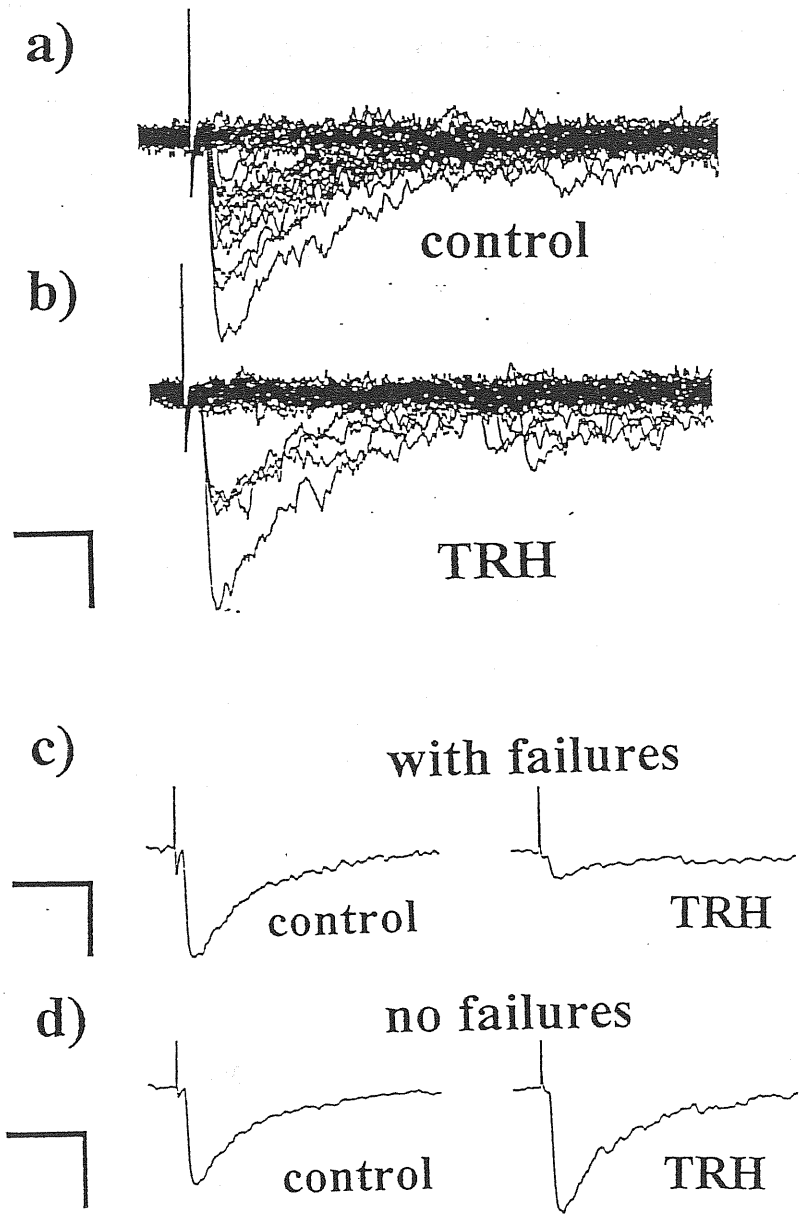
a)
control
b)
TRH
c)
with failures
control
TRH
d)
no failures
control
TRH

Fig.22 Effect of TRH on ePSCs

a) and b) show the first 20 superimposed raw traces before and after bath-application of 10 μM TRH (in the presence of 1 mM kynurenic acid). For these responses the latency from the stimulus artifact is 4.5 ms, rise- and decay-time are about 1.5 ms and 24 ms respectively. Calibration bars: 20 ms, 150 pA. c): averaging over 50 responses (including failures) yields a mean amplitude of 88±106 pA in control vs. 20±87 pA in 10 μM TRH. Calibration bars: 40 ms; 60 pA. d): after excluding failures from averages it is clear that TRH does not depress evoked responses. The number of failures raises from 28/50 in control solution to 42/50 in TRH solution. Calibration bars: 40 ms; 160 pA.

Chapter 6

Modulation of GABAergic activity by $[Cl^-]_i$: effect of Cl^--transporter blockers

The effect of the variation in $[Cl^-]_i$ was studied by analyzing the changes in the characteristics of GABAergic sPSCs. Since in the CA3 area the frequency of sPSCs is higher than in CA1, the CA3 region was chosen for this patch-clamp study. Pyramidal cells were the ones selected for this investigation, in which the intracellular solution Intra1 was used. In this series of experiment sPSCs had an average frequency of 0.86±0.30 Hz and a mean amplitude of 18.1±4.7 pA (n=27).

6.1 Effect of furosemide

6.1.1 Spontaneous currents

The most striking effect caused by the application of 1 mM furosemide was that it increased the frequency of sPSCs from 0.97±0.20 to 1.67±0.38 Hz (n=11), as shown in the example of fig.23, a. In some experiments such an effect was reproduced up to 6 times on the same cell. The effect was reversible and dose dependent, with an apparent dissociation constant K_d = 0.87±0.08 mM (fig.24, a), calculated by fitting the experimental data to a dose-frequency response function of the form:

$$\Delta f = \Delta f_o \, [\, 1 + (K_d/C)^n]^{-1} \quad ,$$

where Δf is the frequency variation, Δf_o is the maximal obtainable variation, C concentration of furosemide and n the Hill coefficient.

The cumulative distribution of inter-event interval is shown in fig.23, c, for a typical cell in control and after furosemide treatment.When furosemide was applied for 2-4 minutes a complete recovery was usually obtained after ten minutes. Furosemide lowered sPSCs amplitudes (34±5%, n=11, $p<0.05$) and increased the risetime values (28±8%, fig.24, b) with no significant change in the decay times (12±14%). The presence of a postsynaptic effect of furosemide was tested with applications of the $GABA_A$ agonist muscimol. Bath-applied muscimol (100 nM) elicited a sustained inward current (95±12 pA, n=3) and an increase in cell conductance (24±11 %, n=3). Furosemide application (3 minutes before muscimol) produced a statistically significant ($p<0.05$) reduction (16±5%) in the inward current and a diminuition of the conductance increase (11±6%) induced by muscimol. Full recovery was obtained after 10 minute washout.

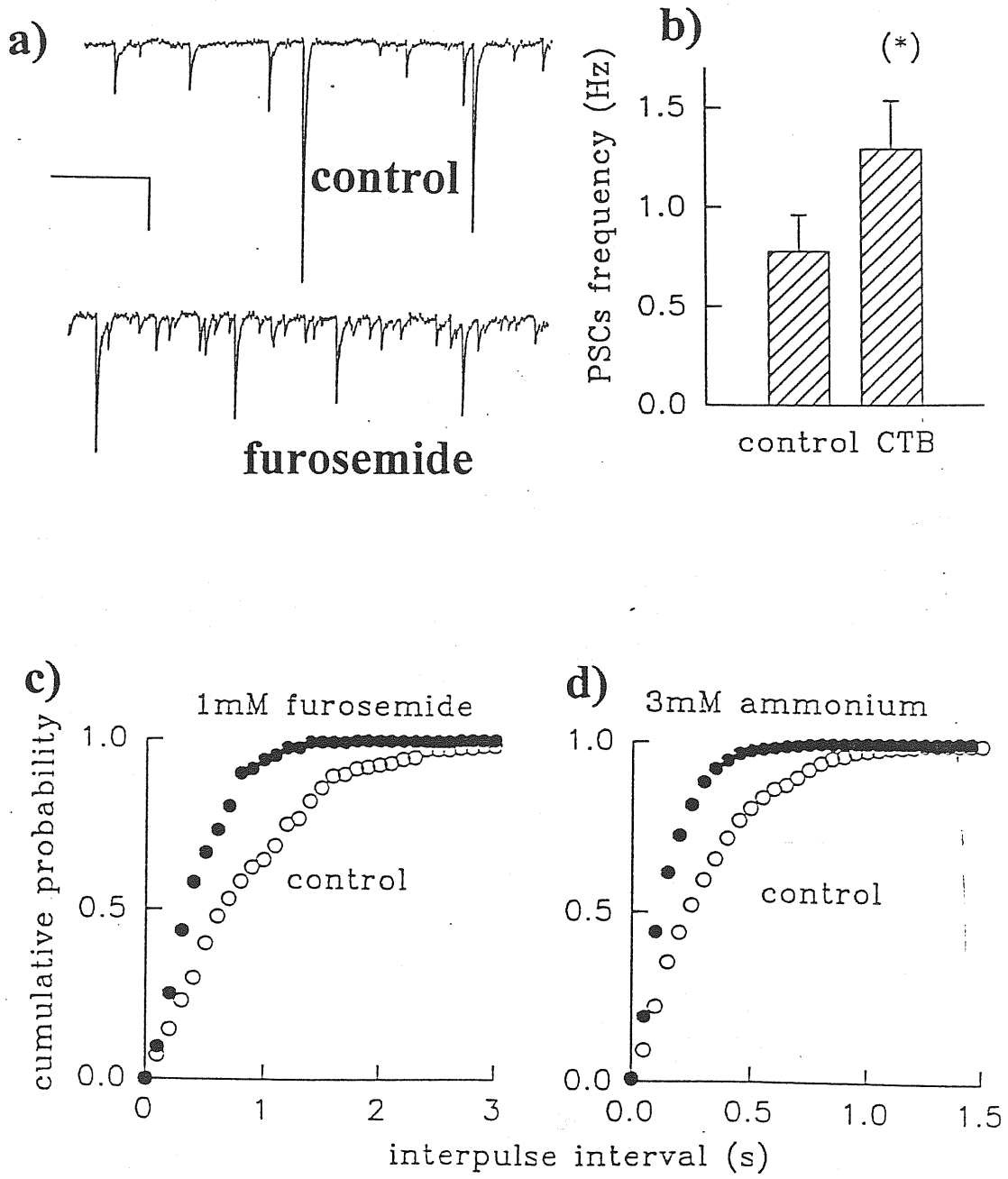
a)
control
furosemide
b)
(*)
PSCs frequency (Hz)
1.5
1.0
0.5
0.0
control CTB
c)
1mM furosemide
cumulative probability
1.0
0.5
0.0
control
0
1
2
3
d)
3mM ammonium
1.0
0.5
0.0
control
0.0
0.5
1.0
1.5
interpulse interval (s)

Fig. 23 Effect of chloride-transporter-blockers on spontaneous PSCs

a) above: control recording ; below recording after 150 s application of 1 mM furòsemide. Calibration bar: 2 s, 40 pA.

b) variation of frequency after treatment with chloride transporter blockers: control conditions vs. treatment (CTB; n=22). The asterisk (*) indicates that the differences from the control values are statistically significant with $p<5\%$. The frequencies were calculated over time spans from 2 to 5 min in order to have at least 100 events per epoch.

c) and d) effect of furosemide and ammonium ions: cumulative frequency histograms before (open circles) and after (filled circles) the treatment with 1 mM furosemide and 3 mM ammonium ions respectively, for single representative cells.

6.1.2 Evoked currents

The effect of furosemide was tested also on evoked PSCs. In 3 experiments ePSCs were evoked by stimulation of SR of CA3 (see fig. 25). The mean latency of the PSCs was 4.4 ± 0.6 ms. Mean amplitude of the ePSC in control was 173 ± 116 pA with 17 ± 4 % of failures. After application of 1 mM furosemide the amplitude of the ePSCs decreased to 111 ± 93 pA and the failures increased to 35 ± 9 %. The decrease in amplitude of the ePSCs could in principle be due to a postsynaptic effect. However, when recalculating the mean amplitude eliminating the failures, the amplitude decreased from 217 ± 93 pA in control to 180 ± 89 in 1 mM furosemide, confirming that furosemide probably induced a postsynaptic downregulation of GABAergic ePSCs.

6.2 Effect of ammonium

Ammonium was also used as chloride transport blocker. Two-three minutes after 3 mM NH_3Cl application an increase in the frequency of sPSCs was detected (58±19%, n=11, fig.24,d), similar to that obtained with furosemide (72±23%).

The increase in frequency induced by ammonium did not significantly affect mean amplitude, rise or decay time of the GABAergic sPSCs. Recovery was not complete following 3mM NH_3Cl application even after 20 minute washout. The mean variation in sPSCs frequency following the application of furosemide or NH_3Cl (n=11 in each case) is shown in fig. 23, b.

a)

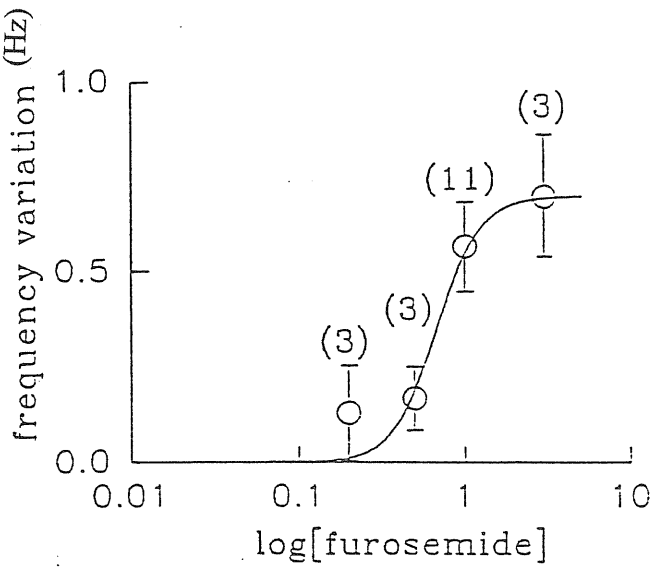
frequency variation (Hz)
1.0
0.5
0.0
0.01
0.1
1
10
log[furosemide]
(3)
(3)
(11)
(3)

b)

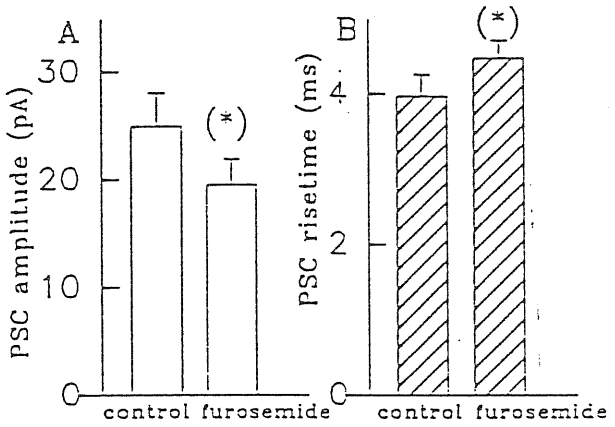
A
PSC amplitude (pA)
30
20
10
0
(*)
control furosemide
B
PSC riseltime (ms)
4
2
0
(*)
control furosemide

c)

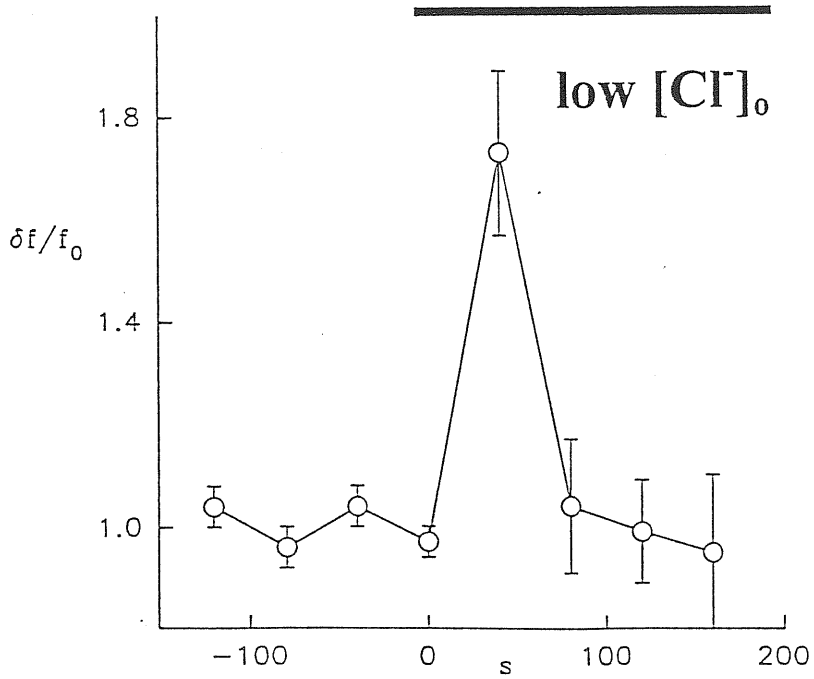
low [Cl⁻]o
δf/f0
1.8
1.4
1.0
−100
0
s
100
200

Fig. 24

a) furosemide dose frequency-response curve

Each point represents the average variation of the frequency for n (indicated above each point) vs. the logarithm of the concentration of furosemide. Mean ± s.e.m. are reported. The curve has been fitted with the expression $\Delta f = \Delta f_o \, [\, 1 + (K_d/C)^n]^{-1}$, with Δf frequency variation, Δf_o maximal obtainable variation, K_d dissociation constant, C concentration of furosemide and the Hill coefficient, yielding the values of $K_d = 0.67 \pm 0.08$ mM and $n = 3.3 \pm 1.0$.

b) postsynaptic effect of furosemide

Variation in the mean amplitude (A) and in the mean rise-time (B) of PSCs after application of 1 mM furosemide (n=11). The average amplitude decreases while the mean risetime increases. The asterisk (*) indicates that the differencies with the control values are statistically significant with $p<5\%$.

c) effect of low chloride solution

Timecourse in the variation of the frequency of sPSCs following 50% substitution of external chloride with isethionate. The frequency values are normalized to the average of the steady state level. The frequencies are calculated over an interval of 40 s (n=3).

a)

control

furosemide

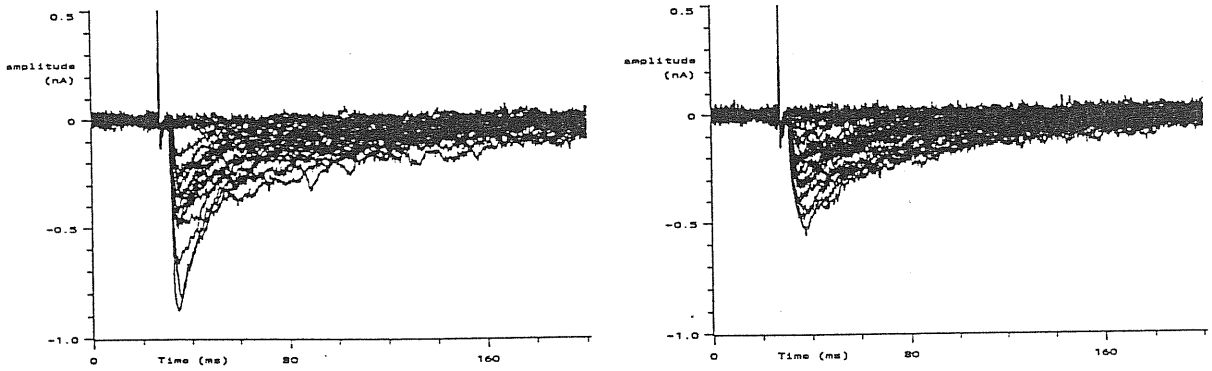

b)

with failures

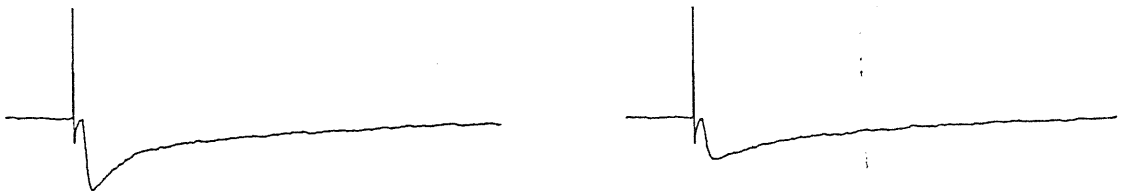

c)

no failures

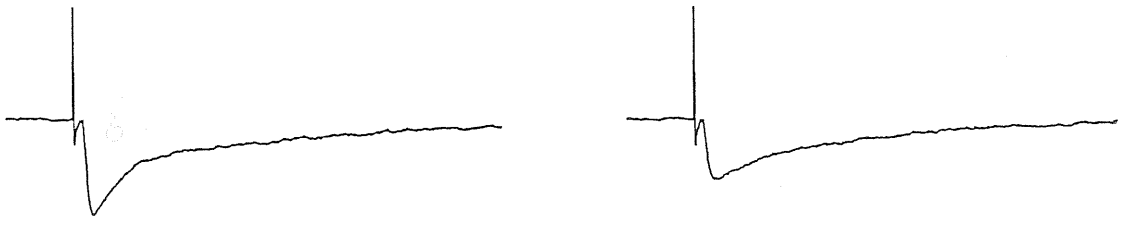

Fig.25 Effect of furosemide on evoked PSCs

Furosemide decreased the mean amplitude of the evoked PSCs:

a) 20 traces evoked by stimulation of the Stratum Lacunosum-Moleculare. Control traces are on the left, traces after application of 1 mM furosemide on the right.

b) The mean of the evoked PSCs is reported for the overall acquisition period.

c) The mean of the evoked PSCs is calculated after eliminating the failures.

For b) and c) calibration bar as for a).

Both in b) and in c) the mean amplitude decreases after application of furosemide.

6.3 Exchange of external $[Cl^-]$ or $[K^+]_i$

Changing the chloride reversal potential by 50% substitution of extracellular chloride $[Cl^-]_o$ with isethionate elicited a transient rise in the sPSC frequency (73±16%, n=3, fig. 24, c), followed by a return to the previous (or even lower) frequency. Furosemide applications after lowering $[Cl^-]_o$ did not significantly change sPSCs frequency but rather prolonged the time during which the frequency increase was present (from about 3 minutes to 6-10 minutes). A rise in extracellular $[K^+]$ ($[K^+]_o$) should impair Cl^- transport since CCTs are driven by the $[K^+]$ gradient. Changing $[K^+]_o$ from 3.5 to 10 mM elicited, after about 3 minutes, a transient increase in the sPSCs frequency (118±83%, n=3). No further enhancement was observed after the application of furosemide (1mM). The frequency increase induced by the high $[K^+]_o$ treatment was approximately 3-times larger than the one elicited by previous application of furosemide alone.

6.4 Miniature PSCs

Since glutamatergic inputs were blocked, the increase in frequency of sPSCs might have been elicited by increasing either interneuron firing rate or the mechanism of release itself. To test for the second possibility furosemide and ammonium chloride were applied (n=3 and n=2, respectively) in the presence of 1 μM TTX to eliminate action potential driven release. No significative change in the frequency of miniature PSCs (mPSCs) (0.25±0.04 after treatment vs. 0.29±0.04 Hz in control, n=5) was observed.

Chapter 7

Discussion

7.1 Characteristics of spontaneous GABAergic transmission

The characteristics of spontaneous GABAergic transmission were studied in pyramidal cells of the CA1 and CA3 region of the hippocampus and in interneurons of the CA1 SL-M layer. Rise- and decay-time of the sPSCs did not statistically differ in the three groups of cell suggesting similarity of the correspondent postsynaptic receptors. Differences in the amplitude of sPSCs between CA1 and CA3 could be due to a different number of synaptic $GABA_A$-receptors or to a different electrotonic filtering although the similar kinetics would favour the former interpretation. The slight differencies in the mean frequency may reflect a lower degree of GABAergic connections onto interneurons in respect with pyramidal cells (0.22 Hz), and onto CA1 in respect with CA3 (0.11 Hz), although large individual differences within each single sample do not allow a clear-cut cellular classification on this basis. The interevent interval histograms were adequately fitted by a first order poissonian for recordings from PCs as well as from SL-M INs. If PCs and SL-M INs receive a common input from a distinct class of yet unidentified interneurons, GABAergic activity recorded from PCs or SL-M INs

should display similar modulation by exogenously-applied agonists via a receptor system located on the input interneurons. For this purpose we used substances known to act in completely different ways at cellular level, as reported in chapter 4. These substances shared the property of modifying the frequency of spontaneous GABA release. Furosemide, carbachol and t-ACPD elicited an increase while baclofen and 5-HT caused a decrease in the frequency of sPSCs, indicating an effect on the afferent presynaptic GABAergic interneurons. Bath-application of agonists failed to reveal any differential modulation of sPSCs characteristics in the two classes of neuron: in facts drugs inducing variations in the frequency of sPSCs from pyramidal cells elicited a similar effect on sPSCs recorded from SL-M interneurons. Quantitative differences of drug-induced frequency variation can be accounted for by the limited sample size. The unpaired Student *t*-test comparing the variation of frequency in PCs and in SL-M interneurons was, in fact, non-significant in all cases. It was thus impossible to prove two distinct sources of sPSCs in PCs or in SL-M INs, indicating that the same distinct set of GINs is probably responsible for both responses.

Simultaneous recording from a PC and a SL-M IN revealed a number of synchronous events significantly larger than the number of randomly expected coincidences. The average time lag between correlated events from the two cell types was a fraction of the mean event rise-time, indicating that the correlated events were synchronous within the experimental error. The continous presence of a glutamate receptor blocker suggests that simultaneous events were not caused by co-activation of two distinct GINs by a glutamatergic input. Several possibilities could account for the observed synchronicity of synaptic currents. The first one is that the two cells directly influenced each other but this interpretation would require that the activity of one cell would follow regularly the activity of the other one at constant latency, a fact not borne out by experimental observations. Moreover, as both cells were clamped at -70 mV, their ability to fire action potentials was blocked, thus preventing their cross-communication. A more likely possibility is that the high degree of synchronicity derived from the fact that synaptic responses from each neuron were driven by the activity of a third, distinct GIN or set of interneurons. PCs and SL-M INs seemed thus not only to share an input from a single class of GIN

but even from a single cell or group of cells, giving further support to the hypothesis previously raised that test neuromodulators used acted via the same class of cells.

The existence of several types of GINs is widely accepted (Buhl et al. 1994, Freund et al. 1990). In the CA3 area and in DG the presence of cells identified as GINs projecting across and beyond the layer of principal cells (Han et al. 1993, Gulyás et al. 1993) has been reported, suggesting that interneurons projecting over a large distance are relatively widespread in the hippocampus. Morphologically distinct types of interneurons are present in the three layers of the hippocampal CA1 region: O-A INs, basket and vertical cells in or close to SP INs and SL-M INs.

A body of evidence indicates that SL-M INs, identified as stellate, horizontal and short axon neurons, are positive for GAD staining and thus GABAergic (Ribak et al., 1978). The low level of their spontaneous firing (Lacaille and Schwartzkroin 1988 a) suggests that they give a relatively small contribution to spontaneous GABAergic activity in a slice preparation. On the other hand, GINs of the oriens/alveus layer, which establish inhibitory connections with a number of hippocampal cells including SP neurons and SL-M INs (Bernard and Wheal, 1994), exhibit prominent and persistent spontaneous firing (Lacaille and Williams 1990; Lacaille, 1991) although their sparse location makes difficult to stimulate them with electrical pulses. Such characteristics make them likely candidates as a source for the spontaneous GABAergic activty recorded in PCs and SL-M INs. Electrophysiological evidence for the GABAergic nature of interneurons in O-A and SP is also available (Lacaille et al. 1987, Lacaille and Schwartzkroin 1988 a). These cells show a resting potential more positive with respect to SL-M INs (-51 mV and -55 mV respectively vs. -58 mV, Lacaille et al., 1987). In the hippocampal CA1 area O-A INs show processes crossing SP and SR reaching SL-M (Lacaille and Williams 1990).

The present results suggest the existence of a class of GABAergic interneurons simultaneously projecting to PCs and to SL-M INs. O-A IN together with SP-INs are believed to exert the feed-forward and feed-back inhibition elicited by activation of the primary afferents in the hippocampal slice preparation (Miles and Wong 1987, Lacaille et al. 1987, Lacaille and Schwartzkroin 1988 a,

Lacaille and Williams 1990, Lacaille, Williams and Lacaille 1992). Such a circuitry could shape spatially or temporally neuronal [illegible], mediating recurrent inhibition onto PCs and SL-M INs at the same time, after phasic activ[illegible]PCs. Since spontaneous events occurred at high frequency and were subjected to neurotran[illegible]modulation, a functional role for such a tonic GABAergic spontaneous release seems likely [illegible] view of the fact that bicuculline application negatively shifted the holding current. Spon[illegible]activity might indeed act as a limiter for the overall activity of the feedforward circuit. Since [illegible] is a continuous parameter, cellular excitability could thus be varied by spontaneous GABA[illegible]ivity in a non quantal fashion, allowing a flexible control by different neuromodulators. This [illegible] does not exclude that spontaneous GABA release might also have a role in neuronal [illegible]uidance or synaptic plasticity during the formation of hippocampus functional units du[illegible]elopment. This phenomenon would of course be important in the developing brain tissue like [illegible]used in the present study on neonatal rats.

7.2 TRH modulation [illegible]BA release

We focussed our attention to th[illegible]tion by the endogenously-occurring neuropeptide TRH of pharmacologically-isolated GABA[illegible] mediated transmission on rat hippocampal neurons. TRH was used as a model neuromodu[illegible]order to understand whether uniform changes in GABAergic transmission could be observed f[illegible]ent sources and at different locations. For this purpose two different types of synaptic even[illegible] considered: the spontaneous ones and those obtained by extracellular stimulation of the hip[illegible] afferents. Such experiments were to confirm (or otherwise) the proposal made in the previou[illegible] regarding the widespread output of a subset of GABAergic neurons that generated the sponta[illegible]nts. A differential action by TRH on evoked or spontaneous PSCs may simply reflect distinct[illegible] targets for the action of the peptide rather than dissimilar

sensitivity of trasmitter release mechanisms within the same cell type. Thus, TRH might regulate the excitability of pyramidal cells via different GABAergic cells to depress or augment specific inhibitory inputs. GABAergic transmission indeed was not uniformly affected by TRH since sPSCs were enhanced in their frequency while electrically-evoked PSCs were on average depressed.

7.2.1 Effects of TRH on spontaneous PSCs

TRH elicited a persistent, large increase in the frequency of sPSCs of pyramidal cells as well as of SL-M interneurons. Since the frequency of mPSCs in TTX solution was not enhanced by TRH, a direct involvement of TRH in the mechanisms of GABA release is unlikely. In most cells the increased sPSC frequency was not accompanied by changes in the amplitude of the postsynaptic currents. Furthermore, there was no effect of TRH on baseline current and input conductance. All these observations thus suggest that the action of TRH was predominantly presynaptic at the level of the action potential-dependent release of transmitter by GABAergic interneurons. Occasional increase in the amplitude of the GABAergic currents were observed in a subset of cells. The large amplitude increase measured in those cells suggests that a quiescent set of neurons with large quantal content (presumably different from the set active at rest) had been recruited. The frequency of sPSCs in mini-slices lacking the dentate gyrus, the CA3 region (or both) demonstrated that TRH-sensitive neurons projecting to CA1 PCs and SL-M INs were localized within the CA1 area itself. In simultaneous measurements of synaptic activity from pyramidal neurons and SL-M interneurons the frequency of the spontaneous events in each cell, as well as the number of coincident events from two cells, were raised, as expected, by the application of TRH, as well as the number of coincident events, but the ratio between randomly expected and measured concurrences of synaptic events remained unchanged, indicating that the peptide did not change the degree of functional coupling between these two cells. Synaptic responses from each neuron were likely

driven by the activity a the subset of GINs, probably those of the O-A layer, sensitive to TRH. This proposal accords with the similarity of the characteristics of sPSCs from pyramidal neurons and SL-M interneurons (see fig. 9 and tab.3) and with the observation that a similar frequency modulation is induced by the application of furosemide, carbachol, t-ACPD, l-arg, baclofen and 5HT (see fig. 14). A comment may be added on the tachyphylaxis of the effects of TRH which, once developed, required a long recovery (about 30 min). It seems probable that tachyphylaxis was not the result of whole cell dialysis by the patch pipette in view of the response recovery, but it might have been due to changes in the signal transduction mechanisms mediating the action of TRH (Gershengorn, 1986) as previously discussed for other central neurons recorded with sharp microelectrodes (Fisher and Nistri, 1993).

7.2.2 TRH-induced rhythmic PSCs

Even though large amplitude GABAergic rhythmic events were detected only in a minority of cells, it seemed of interest to observe that TRH was able to elicit them. The rhythm of such oscillatory PSCs (about 2 Hz at room temperature) was near the lower values (4 Hz) of the hippocampal theta rhythm of *in vivo* animals (Ylinen et al, 1995), especially when considering the large disparity in temperature. Although the theta rhythm is traditionally supposed to be dependent on the cholinergic projection from the septal area (Petsche et al, 1962) which is modulated by TRH (Lamour et al, 1985), it seems that GABAergic interneurons of the hippocampus are important to shape it (Stewart and Fox 1990; Ylinen et al., 1995). The complex circuitry underlying the generation of theta rhythm prevents the use of the hippocampal slice as a suitable model for theta oscillations. Nevertheless, at least in the cases found in the present study, TRH could trigger GABAergic rhythmic oscillations even after severance of septal afferents in the process of preparing the slices.

7.2.3 Effects of TRH on the evoked PSCs

In the presence of kynurenic acid, focal stimulation applied to the SL-M area elicited (after constant delay) bicuculline-sensitive short-latency (probably monosynaptic) PSCs recorded from PCs. The stimulus intensity was adjusted to activate only a very small number of fibres (possibly only one fiber, "minimal stimulation") as judged by the high rate of failures. In this case, the variability in the size of the ePSC depends on the random number of vesicles released at every active site by the constant stimulation, and its response, averaged over a sufficiently large number of events, is constant in time. Although the hippocampus provides severe technical challenges to a reliable quantal analysis, such a method has been applied to excitatory synaptic transmission in the slice preparation, where regularly spaced peaks have been obtained in the ampitude histograms (Jonas et al., 1993). On the other hand, quantal analysis of GABAergic synaptic transmission often displays irregularly spaced peaks in the amplitude histograms in hippocampus (Edwards et al., 1993) as well as in low-noise preparations (Borst et al., 1994). The lack of a definite, unique, quantal size in the amplitude histograms of the evoked GABAergic currents represents a serious drawback in order to pursue a reliable quantal analysis since it also suggests possible differences in quantal content and in release probability between the different active sites. The dishomogeneity in the quantal parameters would require introduction of a number of model parameters disproportionately large (3 per each active site) with respect to the precision of the experimental histograms, which are limited by electrical noise as well as by the maximum number of responses obtainable in stable conditions. In order to avoid the uncertainty of these experimental methods the present study used simple measurements which, nonetheless, allowed to obtain important information with a relatively straightforward analysis. The observed variation in the number of failures indicates a modulation of the release at a presynaptic level, while a variation in the amplitude without changes in the number of failure may possibly be due to postsynaptic causes (Voronin, 1993). In our case, the mean amplitude of a large number (usually 50) of PSCs was depressed after application of TRH. The changes in PSCs amplitude were merely due to the

increased number of failures of GABAergic currents as all the other parameters pertaining to these responses were essentially unaltered by TRH. Against the hypothesis that TRH directly inhibited the membrane excitability of SL-M interneurons stand the findings obtained with direct recording from the interneurons, in which no inhibitory action by TRH could be demonstrated in terms of variations in baseline current or input conductance. In TRH solution the increased frequency of sPSCs indicated that the GABAergic input received by these cells was actually enhanced. This suggests an indirect action by TRH, namely that the higher number of failures of sPSCs observed in pyramidal cells was probably due to the increase in background inhibition impinging upon GABAergic SL-M INs which reduced their firing probability and thus GABA release onto pyramidal cells.

7.2.4 Cellular mode of action of TRH

The effects of TRH on a large variety of cells ranging from pituitary cells (Geshengorn, 1986) to brain neurons (Toledo-Aral et al., 1993) appear to be due to activation of intracellular second messenger pathways leading to formation of inositol-triphosphate and activation of protein kinase C. These events produce a transient rise in intracellular free Ca^{2+}. It is difficult to translate these effects into the observed enhancement of spontaneous GABAergic activity particularly because the identity of the TRH-sensitive neurons remains elusive. On pyramidal cells (Ballerini et al, 1994), septal neurons (Toledo-Aral et al, 1993) and pituitary cells (Bauer et al., 1990; Kramer et al., 1991) TRH can depress various K^+ conductances which contribute to inhibition of spike generation. One might suspect that, if a similar suppression of intrinsic K^+ conductances by TRH took place in a subset of GINs, the excitability of such cells and consequently their spike-dependent release of GABA would be enhanced. This phenomenon might have functional relevance to the operation of the network comprising CA1 PCs particularly since it may help to complement the TRH-induced increase in NMDA receptor mediated synaptic transmission (Stocca and Nistri, 1995).

7.3 Modulation of GABA release by changes in $[Cl^-]_i$

Finally, to address the problem of whether $[Cl^-]_i$ influenced the behaviour of GABAergic interneurons Cl^--pump blockers were applied to the preparation in the presence of glutamate receptor blockers. Bath application of furosemide reversibly enhanced sPSC mean frequency. The K_d value ($K_d = 0.67 \pm 0.08$, fig. 24a) was similar to that found for a low affinity binding site for furosemide in the rat brain synaptosome preparation (Babila et al., 1989; $K_d = 0.68$ mM). Since the block of glutamate receptors by kynurenate eliminated the main excitatory input, the frequency increase induced by furosemide on sPSCs was likely due to an enhancement in the activity of the interneurons directly impinging on PCs. Mean amplitude and risetimes of the GABAergic sPSCs also changed significantly after furosemide applications. While the frequency variation was certainly a presynaptic effect, the variation in the mean amplitude and risetime may be explained by a partial block by furosemide of the response to GABA. This phenomenon could also indirectly affect the excitability of interneurons. Such effects of furosemide on the GABA-receptor were already described in vertebrate (Nicoll, 1977) and invertebrate (Katchman and Zeimann, 1987) neurons as well as in hippocampal slices (Pearce, 1993). The reduction of the response to exogenous muscimol after furosemide application confirmed such findings.

In order to block chloride transport (with no apparent effect on $GABA_A$ receptors) ammonium ions were used. Bath application of 3 mM NH_3Cl increased the frequency of GABAergic sPSCs with no appreciable effect on amplitude or risetime. These results indicate that the ability of furosemide to block CCT and to change $[Cl^-]_i$ was probably responsible for the increase in sPSC frequency. Two mechanisms determine the intracellular concentration of Cl^- : passive Cl^- flow (through leak Cl^--selective pores and GABA channels opened by the sPSCs) and Cl^- transport via CCT (Zhang et al.,

1991). The former regulates $[Cl^-]_i$ in the first postnatal week (PN 2-5) whereas the latter prevails in the adult animal (PN 15-20). The present data are comparable with those obtained by Zhang et al. for the intermediate pool of cells PN 8-13. At this developmental stage both mechanisms seem to determine $[Cl^-]_i$: according to the Goldman-Hodgkin-Huxley equation the presence of a Cl^- passive conductance leads the Cl^- reversal potential (E_{Cl-}) to contribute to the interneuron resting potential (V_r) proportionally to the cell Cl^- conductance itself. Through this mechanism, in physiological conditions, CCTs mantain a low interneuronal excitability establishing a transmembrane $[Cl^-]$ gradient. The action of CTBs would disrupt of the $[Cl^-]$ gradient restoring thus a higher excitability. Moreover, the fall of the Cl^- gradient induced by Cl^--Transporter-blockers (CTBs) would decrease the effectiveness of the tonic, chloride-mediated inhibition present onto the presynaptic interneurons (Lacaille et al., 1989) thus lowering their firing threshold. Such an interpretation would be in agreement with studies on the cat motor cortex (Raabe and Gumnit, 1975). Another possibility that does not exclude the previous one is that the variations in the chloride reversal potential induced by CTBs directly affected interneuronal V_r. V_r is in fact determined by the resting permeability to different ions, including chloride. This view was confirmed by the fact that a positive shift of the chloride reversal potential by partial substitution of extracellular chloride ($[Cl^-]_o$) with isethionate elicited a transient increase in sPSC frequency. The short duration of the activity enhancement elicited by lowering $[Cl^-]_o$ was probably due to a redistribution of $[Cl^-]_i$ due to passive flow and active transport. Furosemide application after low $[Cl^-]_o$ treatment did not increase sPSC frequency but prolonged the period in which sPSC frequency was enhanced, as expected CCTs contributed to V_r in a hyperpolarizing direction. The increase in the frequency of sPSCs following the elevation of $[K^+]_o$ was mostly due to membrane depolarization, but was also partly due to the block of CCTs, since a further increase in the sPSC frequency following application of furosemide in high $[K^+]_o$ was not observed. CTBs could affect directly GABA release, through a change in $[Cl^-]_i$ inside the axonal terminals. This possibility seems unlikely since block of action potentials by TTX prevented a CTB-

induced increase in mPSCs frequency. Like in the case of TRH, the enhancement in the frequency of sPSC was associated with a decrease in the mean amplitude of the evoked PSC, further confirming the hypothesis that GABAergic afferents to pyramidal cells are tonically inhibited by spontaneously active afferents.

7.4 A possible role for hippocampal GABAergic interneurons

In spite of the wealth of information available about the biophysical and synaptic properties of GABA-receptors and GABA release, the physiological role of the GABAergic hippocampal circuitry is still far from being understood. Clinical studies on human epilepsy and some animal models give some hints on the function the GABAergic system might have: excitation in the absence of inhibition tends to generate loops of oscillating activity leading in turn to seizures. Nevertheless, a general malfunctioning of the GABAergic system, such as that induced in experimental animals by application of GABA receptor blockers or by kindling, cannot be considered as the explanation for the action of the GABAergic circuitry in the same way observations on brain lesions do not necessarily explain the function of the damaged region. In order to explain hippocampal GABAergic circuitry an analogy with the neocortex may be adopted. The neocortex is believed to use two broad classes of interneuron: stellate cells and basket cells. The columnar organization of neocortex prompts a hypothesis on the function of the two classes of interneuron: stellate cells would receive an extracortical input and would carry a feedforward inhibition onto pyramidal neurons of their own column while basket interneurons would cause columns to work in relative isolation from each other (Martin, 1991). Basket and stellate interneurons are certainly present in the CA1 and CA3 regions of the hippocampus, where stellate cells are believed to carry out feedforward inhibition whereas basket cells are traditionally believed to elicit both feedforward and feedback inhibition.The structural organization of neocortex differs from the hippocampal one and since the hippocampal structural unit

is the *lamella*, it seems reasonable to hypothesize a different connection for interneurons within the same *lamella* or between different *lamellæ*. Hence, stellate interneurons would supply each *lamella* with inhibition coming from extrahippocampal areas while basket cells inhibiting a *lamella* would receive their excitatory input from adjacent *lamellæ* and send their axons possibly to all types of neuron within the *lamella*. Our results are compatible with the hypothesis that the hippocampus would be wrapped by an inhibitory network represented by basket cells, highly susceptible to modulation by neurotransmitters influencing the behaviour of both excitatory and inhibitory cells. On the other hand, stellate cells *per se* may be less sensible to neuromodulators, but are indirectly modulated by basket cells, and elicit postsynaptic inhibition just after phasic activation of the afferents onto them. Neuromodulators can thus modify the overall number of interacting hippocampal units or *lamellæ* without interfering with the extrahippocampal input. A diagram of the CA1 region is drawn in fig.26.

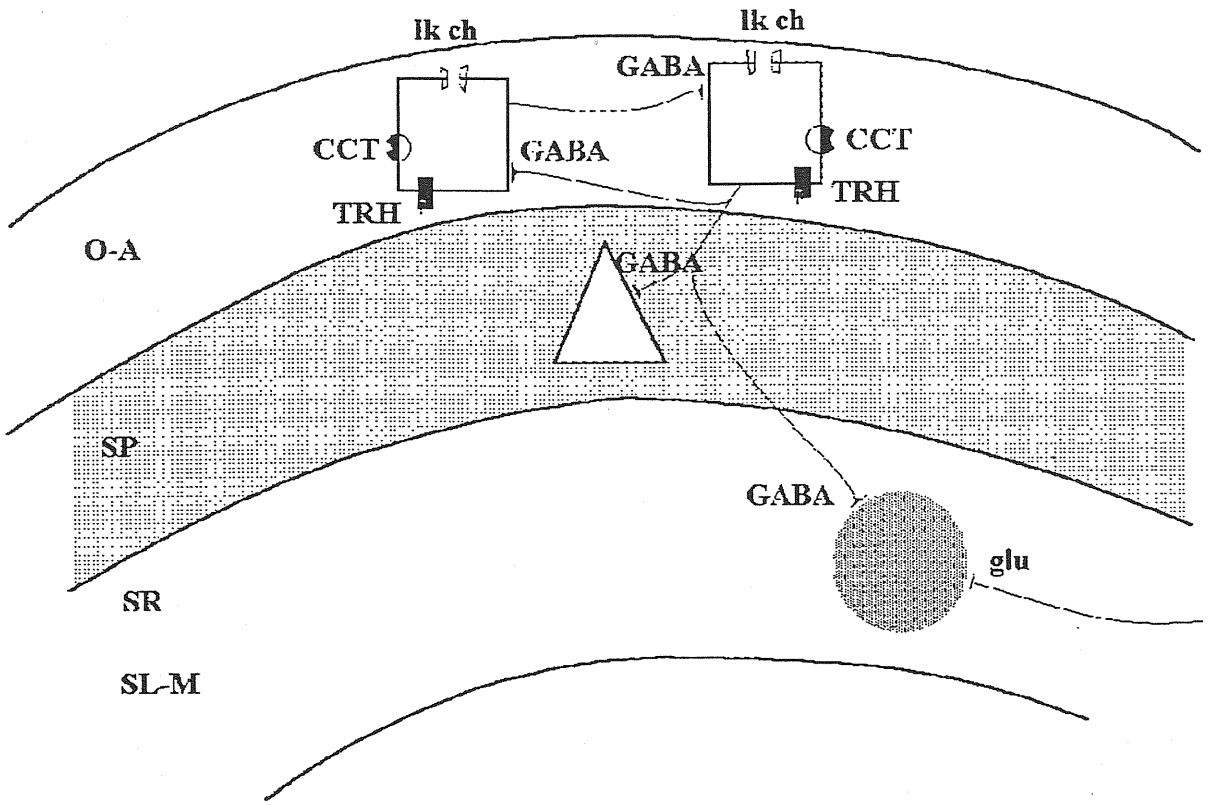

Fig.26: Scheme of the connections considered during the present work in which we show the scheme of the neuronal types involved in the modulation of the GABAergic transmission, the localization of the molecular sites of action of some of the substances used and their possible connectivity. O-A, SP, SR and SL-M indicate the layers Oriens-Alveus, Stratum Pyramidale (shaded), Stratum Radiatum and Stratum Lacunosum-Moleculare respectively. The presence of two types of GABAergic interneurons can account for the present data. The triangle represents a pyramidal cell body while the squares and the circle represent interneurons. GABA and glu indicate GABAergic and glutamatergic synapses respectively, TRH indicates the presence of the TRH receptor, CCT indicates Cl^--Cation-Transporters, lk. ch. indicates the Cl^- leak channels. A set of GABAergic terminals that is activated by extracellular stimulation gives rise to potentials that are down-regulated by TRH while the set of neurons that is the source of the spontaneous GABAergic activity is up-regulated by TRH. Since the spontaneously active interneurons project both to pyramidal cells and to SL-M interneurons which mediate feed-forward inhibition to pyramidal cells, it is likely that the increase in the tonic TRH-induced enhancement of inhibition increases the number of GABAergic failures onto pyramidal cells.

Conclusions

GABAergic transmission in the rat hippocampal slice was investigated with the patch-clamp technique. The main results may be synthesized as follows:

1) Pyramidal cells of the principal regions and interneurons of the Stratum Lacunosum-Moleculare share a GABAergic afference which is normally active at rest and is modulated in a homogeneous manner by substances acting through different cellular pathways.

2) The hormone TRH produces a differential modulation of the GABAergic transmission enhancing the frequency of the tonic release of GABA and decreasing the amplitude of the currents evoked by stimulation of the hippocampal afferents. Two different synaptic pathways can thus be classified on the basis of their up- or down-regulation in response to TRH.

3) Changes in the internal $[Cl^-]_i$ affect the excitability of GABAergic interneurons by varying their resting potential or by reducing the amplitude of the chloride-mediate inhibition.

References

Alger B.E. and Nicoll R.A. (1980) Spontaneous inhibitory postsynaptic potentials in hippocampus: mechanism for tonic inhibition. Br. Res. 200, 195-200.

Alger B. E. and Nicoll R.A. (1982) Feed-forward dendritic inhibition in rat hippocampal cells studied in vitro. J. Physiol. 328, 105-123.

Andrade R. and Nicoll R.A. (1987) Pharmacologically distinct actions of serotonin on single pyramidal neurones of the rat hippocampus recorded in vitro. J. Physiol. 394, 99-124.

Ashwood T.J., Lancaster B. and Wheal H.V. (1984) In vivo and in vitro studies on putative interneurones in the rat hippocampus: possible mediators of feed-forward inhibition. Brain Res. 293, 279-291.

Atzori M. (1994) Cl- transporter block enhances GABAergic spontaneous activity in rat hippocampal CA3 cells. Neuroreport 5, 2509-2512.

Babila T., Gottlieb Y., Lutz R.A. and Lichtstein D. (1989) A bumetanide-sensitive, potassium carrier-mediated transport system in excitable tissues. Life Sciences 44, 1665-1675.

Ballerini L., Corradetti R., Nistri A., Pugliese A.M. and Stocca G. (1994) Electrophysiologic interactions between 5-hydroxytryptamine and thyrotropin releasing hormone on rat hippocampal CA1 neurons. Eur. J. Neurosci. 6, 953-960.

Barker J. and Ransom B.R. (1978) Amino acid pharmacology of mammalian central neurones grown in tissue culture. J. Physiol. Lond. 280, 331-354.

Bayliss D.A., Viana F. and Berger A.J. (1992) Mechanisms underlying excitatory effects of thyrotropin releasing hormone on rat hypoglossal motoneurons in vitro. J. Neurophysiol. 68, 1733-1745.

Bauer C.K., Meyerhof W. and Schwarz J.R. (1990) An inwardly-rectifying K^+ current in clonal rat pituitary cells and its modulation by Thyrotropin-releasing hormone. J. Physiol. 429, 169-189.

Ben Ari Y., Cherubini E., Corradetti R. and Gaiarsa J.L. (1989) Giant synaptic potentials in immature rat CA3 hippocampal neurones. J. Physiol. 416 , 303-325.

Bernard C. and Wheal H.V. (1994) Model of local connectivity in CA3 and CA1 areas of the hippocampus. Hippocampus 4, 497-529.

Bernardi G., Marciani M.G., Morocutti C. and Giacomini P. (1976) The action of picrotoxin and bicuculline on rat caudate neurons inhibited by GABA. Br. Res. 102, 379-384.

Betz H. (1992) Structure and function of inhibitory glycine receptors, Quart. Rev. of Bioph. 25, 381-394.

Bianchi R. and Wong R.K.S. (1994) Carbachol-induced synchronized rythmic bursts in CA3 neurons of Guinea pig hippocampus in vitro. J. Neurophysiol. 72, 131-138.

Borst J.G.G., Lodder J.C. and Kits K.S. (1994) Large amplitude variability of GABAergic IPSCs in melanotropes from Xenopus laevis: evidence that quantal size differs between synapses. J. Neurophysiol. 71, 639-655.

Bowery N.G., Hill D:R. Hudson A.L., Doble A., Middlemiss D.N., Shaw J., Turnbull (1980) (-)Baclofen decreases neurotransmitter release in the mammalian CNS by an action at a novel GABA-receptor. Nature 283, 92-94.

Branch C.L. and Martin A.R. (1985) Inhibition of Betz cell activity by thalamic and cortical stimulation. J. Neurophysiol. 21, 380-390.

Buhl E.H., Halashy K. and Somogyi P. (1994) Diverse sources of hippocampal unitary inhibitory postsynaptic potentials and the number of release sites. Nature 368, 823-828.

Carbone E. and Swandulla D. (1982) Neuronal clacium channels: kinetics, blockade and modulation. Prog. Biophys molec. Biol. 54, 31-58.

Cherubini E, Gaiarsa JL and Ben Ari Y (1991) GABA: an excitatory transmitter in the early postnatal life. TINS 14 ,515-519.

Ebihara S. and Akaike N. (1993) Potassium currents operated by thyrotropin-teleasing-hormone in dissociated CA1 dissociated CA1 pyramidal neurones of rat hippocampus. J. Physiol. 472, 689-710.

Eccles J.C., Ito M. and Szentagothai J. (1967) The cerebellum as a neuronal machine. Springer, Berlin.

Edwards F.A., Konnerth A., Sakmann B. and Takahashi T. (1989) A thin slice preparation for patch-clamp recording from neurones of the mammalian central nervous system. Pflügers Archiv. 414, 600-612.

Eymin C., Champier J., Duvernoy J.M., Martin D., Kopp N. and Jordan D. (1993) Distribution of thyrotropin-releasing hormone binding sites: autoradiographic study in infant and adult human hippocampal formation. Brain Res., 605, 139-146.

Fisher N.D. and Nistri A. (1993) A study of the barium-sensitive and -insensitive components of the action of Thyrotropin-releasing hormone on lumbar motoneurons of the rat isolated spinal cord. Eur. J. Neurosci., 5, 1360-1369.

Frank K. and Fuortes M.G.F. (1957) Presynaptic and postsyanptic inhibition of monosynaptic reflexes. Fed. Proc. 16: 39-40.

Fraser D.D. and MacVicar B.A. (1991) Low-threshold transient calcium current in rat hippocampal lacunosum moleculare interneurons: kinetics and modulation by neurotransmitters. J Neurosci., 11, 2812-2820.

Freund T.F., Gulyás A.I., Acsády L., Görcs and Tóth K. (1990) Serotoninergic control of the hippocampus via local inhibitory interneurons. Proc. Natl. Acad. Sci. 87, 8501-8505.

Frosch M.P., Lipton S.A. and Dichter M.A. (1992) Desensitization of GABA-activated currents and channels in cultured cortical neurons. J. Neurosci. 12, 3042-3053.

Gage P.W. and Chung S.H. (1994) Influence of membrane potential on conductance sublevelsof chloride channels activated by GABA. Proc. R. Soc. Lond. 255, 167-172.

Gerber U. and Gawhiler B.H. (1994) $GABA_B$ and adenosine receptors mediate enhancement of the current $I_K(Ca^{2+})$, I_{AHP}, by reducing adenylyl cyclase activity in rat CA3 hippocampal neurons. J. Neurophysiol 72, 2360-2367.

Gershengorn M.C. (1986) Mechanism of thyrotropin releasing hormone stimulation of pituitary hormone secretion. Ann. Rev. Physiol. 48, 515-526.

Gulyás A.I., Miles R., Hájos N and Freund T.F. (1993) Precision and variability in postsynaptic target selection of inhibitory cells in the hippocampal CA3 region. Eur. J. Neurosci. 5,1729-1751.

Ito S. and Cherubini E. (1991) Strychnine-sensitive glycine responses of neonatal rat hippocampal neurones. J. Physiol. 440, 67-83.

Kisvárday Z.F., Beaulieu C. and Eysel U.T. (1993) Network of GABAergic large basket cells in cat visual cortex (Area 18): implications for lateral disinhibition. J. Comp. Neurol. 327, 398-415.

Hablitz J.J. (1992) Voltage-dependence of $GABA_A$-receptor desensitization in cultured chick cerebral neurons. Synapse 12,169-171.

Halasy K. and Somogy (1993) Subdivisions in the multiple GABAergic innervation of granule cells in the dentate gyrus of the rat hippocampus. Eur. J. Neurosci. 5, 411-429.

Hall AC, Bianchini L and Ellory JC in: Keeling D and Benham C,ed. Ion Transport. Academic Press Limit, 1989: 217-235.

Halliwell J.V. and Adams P.R. (1982) Voltage-clamp analysis of muscarinic excitation in hippocampal neurons. Brain Res. 250, 71-92.

Han Z.S., Buhl E.H., Lörinczi Z. and Somogyi P. (1993) A high degree of spatial selectivity in the axonal and dendritic domains of physiologically identified local-circuit neurons in the dentate gyrus of the rat hippocampus. Eur. J. Neurosci. 5, 395-410.

Hosokawa Y., Sciancalepore M., Stratta F., Martina M. and Cherubini (1994) Develpmental changes in spontaneous $GABA_A$-mediated synaptic events in rat hippocampal CA3 neurons E. Europ. J. Neurosc. 6, 805-813.

Jonas P., Major G. and Sakmann B. (1993) Quantal components of unitary EPSCs at the mossy fibre synapse on CA3 pyramidal cells of rat hippocampus. J. Physiol. 472, 615-663.

Kaila K. (1994) Ionic basis of $GABA_A$ receptor channel function in the nervous system, Prog. in Neurobiol. 42, 489-537.

Kasparov S., Pawelzik A. and Zieglgänsberger W. (1994) Thyrotropin-releasing hormone enhances excitatory postsynaptic potentials in neocortical neurons of rat in vitro. Brain Res. 656, 229-235.

Kawaguchi Y. and Hama K. (1987) Two subtypes of non-pyramidal cells in rat hippocampal formation identified by intracellular recording and HRP injection. Brain Res. 411, 190-195.

Kramer R. H., Kaczmarek L.K. and Levitan E.S. (1991) Neuropeptide inhibition of voltage-gated calcium channels mediated by mobilization of intracellular calcium. Neuron, 6, 557-563.

Krnjevic K. (1964), Randic M. and Straughan D.W. (1964) Cortical inhibition. Nature 201, 1294-1296.

Krnjevic K. and Schwartz S. (1967) The action of γ-amino-butyric acid on cortical neurones. Exp. Br. Res. 3, 320-336.

Krnjevic K. (1982) GABA and other transmitters in the cerebellum. In: The cerebellum, New Vistas 532-551.

Kunkel D.D., Lacaille J.C. and Schwartzkroin P.A. (1988) Ultrastructure of Stratum Lacunosum-Moleculare interneurons of hippocampal CA1 region. Synapse 2, 382-394.

Lacaille J.C., (1991) Postsynaptic potential mediated by excitatory and inhibitory aminoacids in interneurons of Stratum Pyramidale of the CA1 region of the rat hippocampal slices in vitro. J. Neurophysiol. 66, 1441-1454.

Lacaille J.C., Kunkel D.D. and Schwartzkroin P.A. (1989) Electrophysiological and morphological characterization of hippocampal interneurons. In The hippocampus-New Vistas, Liss Inc., 1989: 287-305.

Lacaille J.C., Mueller A.L., Kunkel D.D. and Schwartzkroin P.A. (1987) Local circuit interactions between Oriens/Alveus interneurons and CA1 pyramidal cells in hippocampal slices:electrophysiology and morphology. J. Neurosci. 7, 1979-1993.

Lacaille J.C. and Schwartzkroin P.A. (1988a) Stratum Lacunosum-Molecualre interneurons of hippocampal CA1 region. I. Intracellular response characteristics, synaptic responses, and morphology. J. Neurosci. 8(4), 1400-1410.

Lacaille J.C. and Schwartzkroin P.A. (1988b) Stratum Lacunosum-Moleculare interneurons of hippocampal CA1 region. II. Intrasomatic recordings of local circuit synaptic interactions. J. Neurosci. 8, 1411-1424.

Lacaille J.C. and Williams S. (1990) Membrane properties of interneurons in Stratum Oriens-Alveus of the CA1 region of rat hippocampus *in vitro* . Neuroscience 2, 349-359.

Lamour Y., Dutar P. and Jobert A. (1985) Effetcs of TRH, cyclo-(his-Pro) and (3-Me-His2)TRH on identified septohippocampal neurons in the rat. Brain Res. 331, 343-347.

Lonart G., Wang J. and Johnson K.M. (1992) Nitric oxide induces neurotransmitter release fro hippocampal slices. Europ. J. Pharmacol. 220, 271-272.

Low C.L., Roepke J., Farber S.D., Hill T.G., Sattin A. and Kubek M.J. (1989) Distribution of thyrotropin-releasing hormone (TRH) in the hippocampal formation as determined by radioimmunoassay. Neurosci. Lett. 103, 314-319.

Macdonald R.L., Twyman R.E., Ryan-Jastrow T., Angelotti T.P.. (1992) Regulation of $GABA_A$ receptor channels by anticonvulsant and convulsant drugs and by phosphorilation Molecular Neurobiology of Epilepsy. Epilepsy Res. 9 265-277.

Maiewska M.D. (1992) Neurosteroids: endogenous bimodal modulators of the $GABA_A$ receptor: mechanism of action and physiological significance. Prog. in Neurobiol. 38, 379-395.

Manaker S., Winokur A., Rostene W.H. and Rainbow T.C. (1985) Autoradiographic localization of thyrotropin-releasing hormone receptors in the rat central nervous system. J. Neurosci. 1, 167-174.

Martin J.H., The collective electrical behavior of cortical neurons: the electroencephalogram and the mechanisms of epilepsy. In: Principles of neural science, ed. Kandel E.C., Schwartz J.H. and Jessel T.M., New York, Elsevier, 1991.

Mazda J.Y., Nistri A. and Sivilotti L.(1990) The effect of GABA on the frog optic tectum is sensitive to ammonium and to penicillin. Europ. J Pharmacol 179, 111-118.

McBain C. and Dingledine R. (1993) Heteregeneity of synaptic glutamate receptors on CA3 stratum radiatum interneurones of rat hippocampus. J. Physiol. 462, 373-392.

Miles R. and Wong R.K.S. (1987) Inhibitory control of local excitatory circuits in the guinea-pig hippocampus. J. Physiol. 388, 611-629.

Misgeld U., Deisz R.A., Dodt H.U. and Lux H.D. The role of chloride transport in postsynaptic inhibition of hippocampal neurons. Science 232, 1413-1415 (1986).

Müller F., Boos R. and Wässle H. (1992) Actions of GABAergic ligands on brisk ganglion cells in the cat retina. Vis. Neurosci. 9, 415-425.

Newberry N.R. and Nicoll R.A. (1984) Direct hyperpolarizing action of baclofen on hippocampal pyramidal cells. Nature 308, 450-452.

Nicoll R.A. (1978) The block of GABA mediated responses in the frog spinal cord by ammonium ions and furosemide. J. Physiol. 283, 121-132.

Olsen R.W. and Tobin A.J. (1990) Molecular biology of $GABA_A$ receptors The FASEB J. 4, 1469-1480.

Otis, T.S. and Mody, I (1992) Modulation of decay kinetics and frequency of $GABA_A$ receptor-mediated spontaneous inhibitory postsynaptic currents in hippocampal neurons. Neurosci 49, 13-32.

Pearce R.A. (1993) Physiological evidence for two distinct $GABA_A$ responses in the rat hippocampus. Neuron 10, 189-200

Purpura D.P. and Cohen (1962) Intracellular recording from thalamic neurons during recruiting response. J Neurophysiol. 25, 621-635.

Raabe W. and Gumnit R.J. (1975) Disinhibition in cat motor cortex by ammonia. J. Neurophysiol. 38, 347-355.

Reckling J.C. (1990) Excitatory effects of thyrotropin-releasing hormone (TRH) in hypoglossal motoneurons. Brain. Res. 510, 175-179.

Ribak C.E., Vaughn J.E. and Saito K. (1978) Immunocytochemical localization of glutamic acid decarboxilase in neuronal somata following colchicine inhibition of axonal transport. Brain Res. 140, 315-332.

Rolls E.T. and O'Mara S. : Neurophysiological and theoretical analysis of how the primate hippocampus functions in memory. In: Brain Mechanisms and Memory, from neuron to behaviour, ed. by Taketoshi O., Squire L.R., Raichle M.E., Perret D.I. and Fukuda M. , Oxford Univ. Press, 1993.

Ropert N., Miles R. and Korn H. (1990) Characteristics of miniature inhibitory postsynaptic currents in CA1 pyramidal neurones of rat hippocampus. J. Physiol. (1990) 428, 707-722.

Sciancalepore M., Stratta F., Fisher N. and Cherubini (1995) Activation of metabotropic glutamate receptors increase the frequency of spontaneous GABAergic currents through protein kinase A in neonatal rat hippocampal neurons. J. Neurophysiol. in press.

Segovia G., Porras A. and Mora F. (1994) Effects of nitric oxide donor on glutamate and GABA release in striatum and hippocampus of the conscious rat. Neuroreport 5, 1937-1940.

Sharif N.A. (1989) Quantitative autoradiography of TRH receptors in discrete brain regions of different mammalian species. Ann. N.Y. Acad. Sci. 553, 147-175.

Stewart M. and Fox S. (1990) Do septal neurons pace the hippocampal theta rhythm ?. TINs, 13, 163-168.

Sivilotti L. and Nistri A. (1991) GABA receptor mechanisms in the central nervous system. Prog. in Neurobiol. 36, 35-92.

Smith G.B. and Olsen R.W. (1995) Functional domains of $GABA_A$ receptors TIPs 16, 162-168.

Staley K. (1994) The role of an inwardly rectifying chloride conductance in postsynaptic inhibition. J. Neurophysiol. 72, 273-284.

Stern P., Edwards F.A. and Sakmann B. (1992) Fast and slow components of unitary EPSCs on stellate cells elicited by focal stimulation in slices of rat visual cortex. J. Physiol. Lond. 449, 247-278.

Stelzer A. Intracellular regulation of $GABA_A$- receptor function. in Ion channels ed. Takahashi, Plenum press, New York (1992).

Stocca. G. and Nistri A. (1994) Modulation by TRH of NMDA-elicited responses of CA1 neurons of the rat hippocampal slice preparation. Neurosci. Lett. 166, 139-142.

Stocca G. and Nistri A. (1995) Enhancement of NMDA receptor mediated synaptic potentials of rat hippocampal neurons in vitro by thyrotropin releasing hormone. Neurosci. Lett. 184, 9-12.

Thompson S.M., Deisz R.A., Prince D.A. (1988a) Relative contribution of passive equilibrium and active transport to the distribution of chloride in mammalian cortical neurons. J. Neurophysiol. 60, 105-124.

Thompson S.M., Deisz R.A., Prince D.A. (1988b) Outward chloride/cation co-transport in mammalian cortical neurons. Neurosc. Lett. 89, 49-54.

Thompson S.M. and Gahwiler B.H. (1989) Activity-dependent disinhibition. II. Effects of extracellular potassium, furosemide and membrane potential on E_{Cl} J. Neurophysiol. 61, 512-523.

Toledo-Aral J., Castellano A., Ureña J. and López-Barneo J. (1993) Dual modulation of K^+ currents and cytosolic Ca^{2+} by the peptide TRH and its derivatives in guinea-pig septal neurones. J. Physiol. 472, 327-340.

Ylinen A., Soltész I., Bragin A., Penttonen M., Sik A. and Buszáki G. (1995) Intracellular correlates of hippocampal theta rhythm in identified pyramidal cells, granule cells, and basket cells. Hippocampus, 5, 78-90.

Vincent P. and Marty A. (1993) Neighbouring cells communicate via retrograde inhibition of common presynaptic interneurons. Neuron 11, 885-893.

Voronin L.L. (1993) On the quantal analysis of hippcampal long-term potentiation and related phenomena of syanptic plasticity. Neurosci. 56, 275-304.

Williams S. and Lacaille J.C. (1992) $GABA_B$ receptor-mediated inhibitory postsynaptic potentials evoked by electrical stimulation and by glutamate stimulations of interneurons in Stratum-Lacunosum-Moleculare in hippocampal CA1 in vitro. Synapse 11, 249-258.

Williams S., Samulack D.D., Beaulieu C. and Lacaille J.C. (1994) Membrane properties and synaptic responses of interneurons located near Stratum-Lacunosum-Moleculare/Radiatum border of area CA1 in whole-cell recordings from rat hippocampal slices. 71, 2217-2235.

Wisden W. and Seeburg P.H. (1992) $GABA_A$ receptor channels: from subunits to functional entities. Curr. Op. in Neurobiol. 2: 263-269.

Zhang L., Spigelman I. and Carlen P.L. (1991) Development of GABA-mediated, chloride-dependent inhibition in CA1 pyramidal cell neurones of immature rat hippocampal slices. J. Physiol. 444, 25-49.